

PHASE-LOCKED LOOP CONTROL SYSTEMS

A THESIS

SUBMITTED TO

THE FACULTY OF GRADUATE STUDIES

OF

THE UNIVERSITY OF MANITOBA

IN PARTIAL FULFILMENT

OF THE REQUIREMENTS

FOR THE DEGREE

MASTER OF SCIENCE

DEPARTMENT OF ELECTRICAL ENGINEERING

CHRISTOPHER SIU-WAH WOO

JUNE 1977

PHASE-LOCKED LOOP CONTROL SYSTEMS

BY

CHRISTOPHER SIU-WAH WOO

A dissertation submitted to the Faculty of Graduate Studies of
the University of Manitoba in partial fulfillment of the requirements
of the degree of

MASTER OF SCIENCE

© 1977

Permission has been granted to the LIBRARY OF THE UNIVERSITY OF MANITOBA to lend or sell copies of this dissertation, to the NATIONAL LIBRARY OF CANADA to microfilm this dissertation and to lend or sell copies of the film, and UNIVERSITY MICROFILMS to publish an abstract of this dissertation.

The author reserves other publication rights, and neither the dissertation nor extensive extracts from it may be printed or otherwise reproduced without the author's written permission.

ABSTRACT

This thesis describes the design and analysis of a class of control systems which combines both concepts of Integral Pulse Frequency Modulation (IPFM) and phase-locked loops (PLL). This concept was stimulated by Moore's work on motor-speed control using phase-locked loops. The proposed system employs two identical IPFM modulators: one of which modulates the system input and the other modulates the plant output. The modulated plant output is fed back and "compared" with the modulated system input. The "comparison process" generates a plant excitation signal which brings the system into the phase-locked state when other appropriate conditions are satisfied. A state variable analysis is applied to the "phase-locked loop control system (PLLCS)" to investigate the locking conditions. Then, an equivalent sampled-data system is developed to facilitate the stability (locking) analysis of the PLLCS.

ACKNOWLEDGMENTS

The author wishes to express his deep gratitude to Dr. S. Onyshko for suggesting the thesis topic as well as for his valuable guidance and encouragement during the course of this work. The author also wishes to acknowledge the National Research Council for financially supporting this work under Grant No. A8008.

TABLE OF CONTENTS

ABSTRACT	i.
ACKNOWLEDGEMENTS	ii.
CHAPTER 1 INTRODUCTION	1.
1.1 <u>Background</u>	1.
(a) Phase-locked loops (PLL)	1.
(b) Integral Pulse Frequency Modulation (IPFM)	2.
1.2 <u>Motivation</u>	3.
1.3 <u>Outline of Analysis</u>	5.
CHAPTER 2 DESIGN OF A PHASE-LOCKED LOOP CONTROL SYSTEM	6.
2.1 <u>Integral Pulse Frequency Modulation (IPFM)</u>	8.
2.2 <u>Analog Phase Comparator</u>	11.
CHAPTER 3 ANALYSIS OF LOCKING CONDITIONS	18.
3.1 <u>Simulation of phase-locked systems</u>	18.
3.2 <u>Locking conditions</u>	23.
CHAPTER 4 STABILITY	31.
4.1 <u>Stability of a phase-locked system</u>	31.
4.2 <u>Determination of system stability</u>	33.
First Order system	37.
Example 1	41.
Second Order System	44.
(a) Linear plant with two distinct poles	44.
Example 2	49.
(b) Linear plant with a multiple pole of order two	51.
Example 3	56.
CHAPTER 5 SUMMARY AND CONCLUSIONS	59.
BIBLIOGRAPHY	61.

CHAPTER 1

INTRODUCTION

This thesis describes the design and analysis of a control system which incorporates features of both pulsed phase-locked loops (PLL) and integral pulse frequency modulation (IPFM). Both PLL and IPFM concepts have been employed previously in control systems; however, they have not been used jointly.

1.1. Background

(a) Phase-locked loops (PLL)

Phase-locked loops are basically feedback systems whose feedback signals are frequencies rather than the magnitude of a voltage or current. Phase-locked loops have become the major building blocks of many systems. The recent development of thick film technology allows phase-locked loops to be assembled with integrated circuits, and this feature results in an almost limitless number of other possible applications.

Initially, phase-locked loops were used in communications, and there has been a tremendous amount of work done in this area, including the demodulation of information carrier signals, synchronization of line pilots and the tracking of carrier frequencies in multiplex systems. The phase-locked loop concept was proposed in the late 1930's to enable the synchronous reception of two radio signals. Later, the pulsed phase-locked loops idea, where the reference input is a pulse stream rather than a sinusoidal signal, was introduced in television receivers for synchronizing the horizontal and vertical sweep oscillator to the transmitted synchronizing pulses. Narrow band phase-locked receivers have also been used in tracking weak satellite

signals because they offer excellent noise immunity.

Recently, it has been shown (M1) that the pulsed PLL concept can be successfully applied to control systems. Moore (M1) designed a pulsed PLL motor-speed control system, and used an optical encoder assembly to generate a pulse stream whose frequency was proportional to the speed of the motor. These pulses were then compared with a reference signal by a digital phase detector. By locking the pulses into the reference signal, speed accuracies of 0.002 percent were obtained.

(b) Integral pulse frequency modulation (IPFM)

Integral pulse frequency modulation (IPFM) is a pulsed scheme which emits a fixed size pulse whenever the integral value of the analog input reaches the predetermined threshold of the scheme. IPFM has been successfully applied to space vehicle attitude control systems (F1), and adaptive control systems (M3).

The first investigation (M1, L1) of IPFM occurred about fifteen years ago. Since then, IPFM has become the most widely used pulse frequency modulation (PFM) scheme due to its simplicity and ease of implementation.

Previous work on the applications of IPFM is quite extensive. Li(L1) and Meyer (M2) have defined IPFM and investigated its effect in feedback control systems. The application of IPFM to space vehicle attitude control has been made by Farrenkopf, Sabroff and Wheeler (F1). Murphy and West (M3) have applied IPFM in an adaptive outer loop around the basic system to obtain an adaptive autopilot for high performance contemporary military aircraft.

1.2. Motivation

There are several advantages in using pulses for control. Economy and efficiency are two of the important factors. In a case of space vehicle attitude control, for example, the inevitable fuel consumption is reduced substantially if pulse bits, rather than constant thrust, are applied to the space vehicle. Also, more efficient operation can potentially be obtained if a jet specifically designed to deliver small fixed size pulses (such as IPFM produces) is used.

Another advantage is that, in remote control applications, control pulses which are contaminated by noise and distortion can easily be recovered. Control pulses (Fig. 1.2.1(a)) which are transmitted over a long distance along any medium are undoubtedly attenuated and distorted (Fig. 1.2.1(b)). The control signal can be regenerated by pulse repeaters which are placed along the transmission medium. The pulse repeaters emit an undistorted pulse whenever the required level of the incoming signal is detected at the detecting level B of the pulse repeater (Fig. 1.2.1(c)).

The idea of designing a control system using PLL principle was stimulated by Moore's work on phase-locked loop motor speed control. In his work, Moore used fixed time clock pulses to control the speed of the motor. He found that this pulsed PLL technique provided excellent accuracy for the motor speed. Moore's success provided the motivation to further study the application of PLL techniques in control systems.

Most control signals are continuous. Thus, the use of PLL methods must allow for conversion from continuous to pulsed signals. From the previous work, IPFM has been proven advantageous in control systems (L1, M2, F1, M3). Also, it can be used as an analog encoder because it takes an

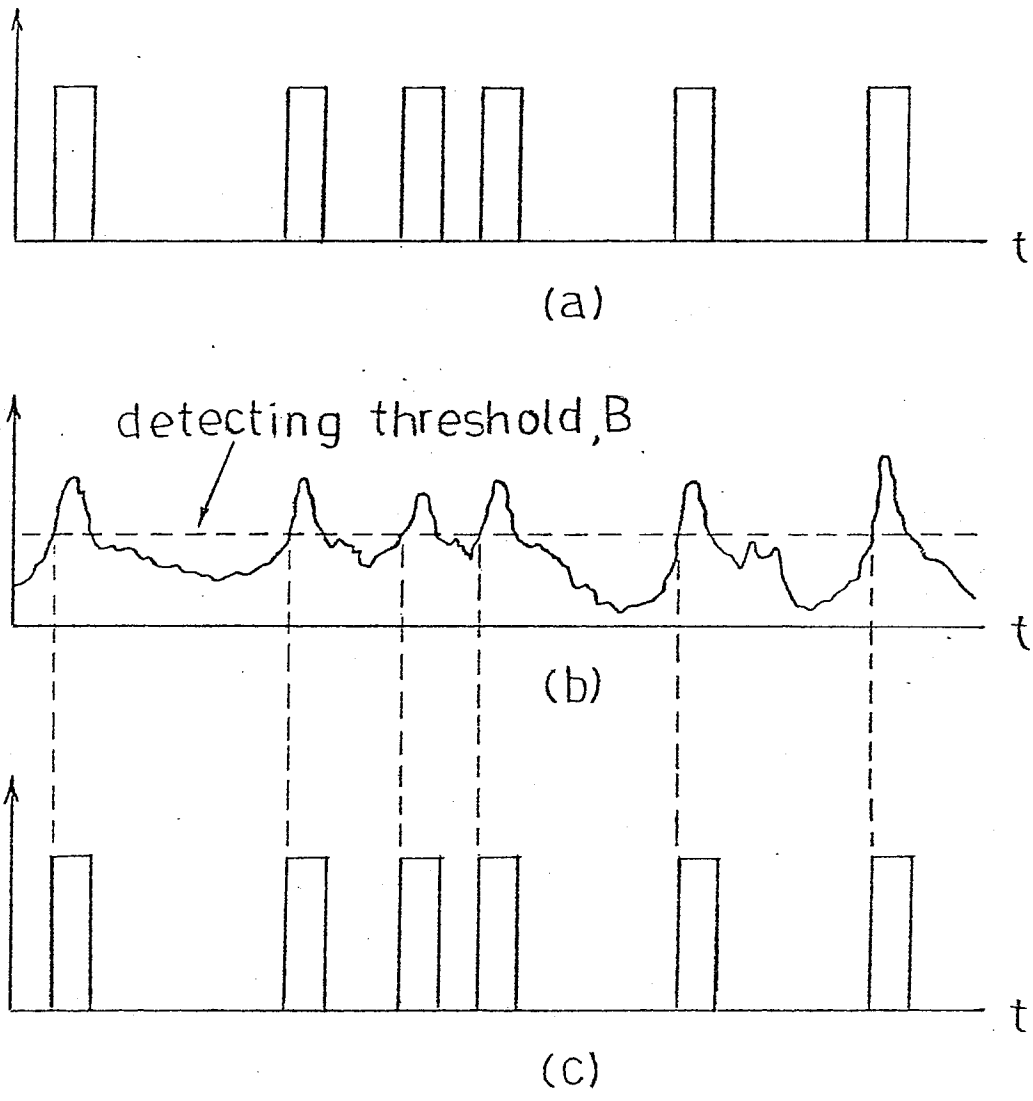


FIGURE 1.21 (a) information pulses
(b) distorted pulses
(c) regenerated pulses

analog signal and converts it into digital pulses. Therefore, the combination of pulsed PLL technique and IPFM may further study the idea that Moore presents in his paper. In this thesis, it is hoped to present a possible PLL - IPFM control system design, and to investigate the locking conditions of such a proposed system.

1.3. Outline of Analysis

The historical background, current status and mode of operation of the phase-locked loops (PLL) and Integral Pulse Frequency Modulation (IPFM) are summarized in Chapter 1. The motivation of designing such a system is due to the drawbacks in Moore's work and the advantages of IPFM in control systems. In Chapter 2, the general concept of a phase-locked system is explained and this new system is compared with the conventional systems. The latter part of Chapter 2 is devoted to the design of the IPFM modulator and the establishment of the analog phase comparator. The mathematical development for the locking system is included in Chapter 3. In Chapter 4, the stability of the system is investigated and is demonstrated for 1st and 2nd order systems. Finally, the conclusions are given in Chapter 5.

CHAPTER 2

DESIGN OF A PHASE-LOCKED LOOP CONTROL SYSTEM

This system is a regulator system. It includes five components; namely, two identical IPFM modulators, an analog phase comparator, an amplifier and a linear plant (Fig. 2.1.1).

The two identical IPFM modulators are used to convert the incoming analog signals into sequences of pulses: one of the IPFM elements modulates the system input signal and the other modulates the plant output. The information originally contained in the system input and the plant output is carried in the spacing between pulses. The spacing is dependent on the relative values of the predetermined threshold value of the IPFM modulator and the incoming analog signal. Larger analog signals give smaller spacings between pulses, and smaller analog signals yield larger spacings.

The analog phase comparator is different from conventional digital phase comparators such as exclusive-or circuits, edge-triggered flip-flop, etc. This analog phase comparator is primarily designed to detect the initiation of the pulse signals of the system input and the plant output. These pulses trigger the logic circuits of the analog phase comparator which, in turn, produces a plant excitation signal. The shape and the magnitude of this plant excitation signal reflects the relative spacing between the initiation time of the associated pulses.

Hence, the proposed system is different from the conventional feedback control system in several aspects. In the conventional feedback system, the system input and the plant output are continuous analog signals. In the proposed system, however, the system input and the plant output are

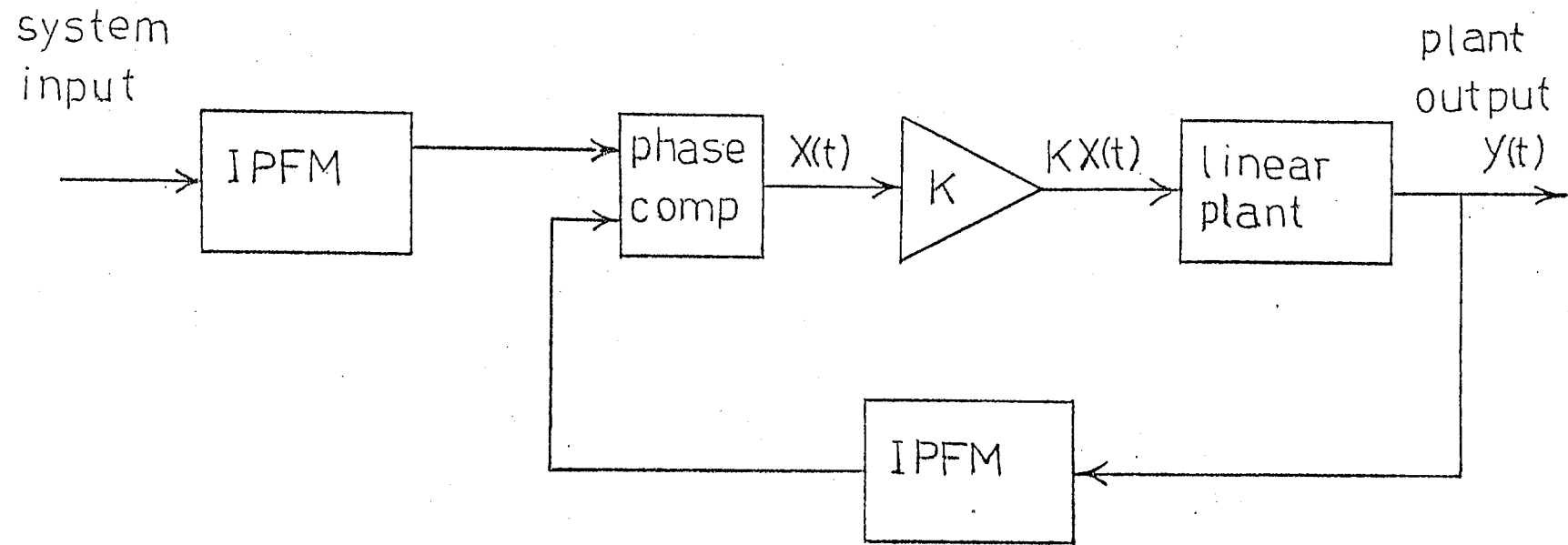


FIGURE 2.1.1 block diagram of a phase-locked loop control system

converted into two sequences of pulses by the two identical IPFM modulators, respectively. Furthermore, the conventional feedback system compares the relative magnitude of the input and output analog signals and produces an error signal which is the difference between the compared signals. In the proposed system, however, an analog phase comparator is designed to detect the initiation of the input and output pulses and to produce an associated plant excitation signal. This plant excitation signal maintains the "phase-locked" system in its steady-state when the locking conditions are satisfied. The "phase-locked" state, as defined in this thesis, is achieved when the two sequences of pulses from the two IPFM modulators interlock with each other.

2.1. Integral Pulse Frequency Modulation (IPFM)

An Integral Pulse Frequency Modulator emits a fixed-area pulse whenever the integral value of its input reaches the positive threshold; the polarity of the pulse is that of the just-encountered threshold. The intervals between successive initiation of pulses contain the information about the modulating signal. The pulses themselves contain no information and are all identical in size and shape.

The schematic diagram of a typical IPFM modulator is given in Fig.

2.2.1. The components include three electronic comparators (i.e. COMP I, COMP II, and COMP III) and an integrator. The operation of these electronic comparators is similar to that of latching relays. When the net input to the comparators as shown in Fig. 2.2.1 is positive, the upper reference signal is switched to the output; otherwise, the lower reference signal is connected through. Also, these comparators invert the polarities of the reference signals: they change the positive signals into negative, and,

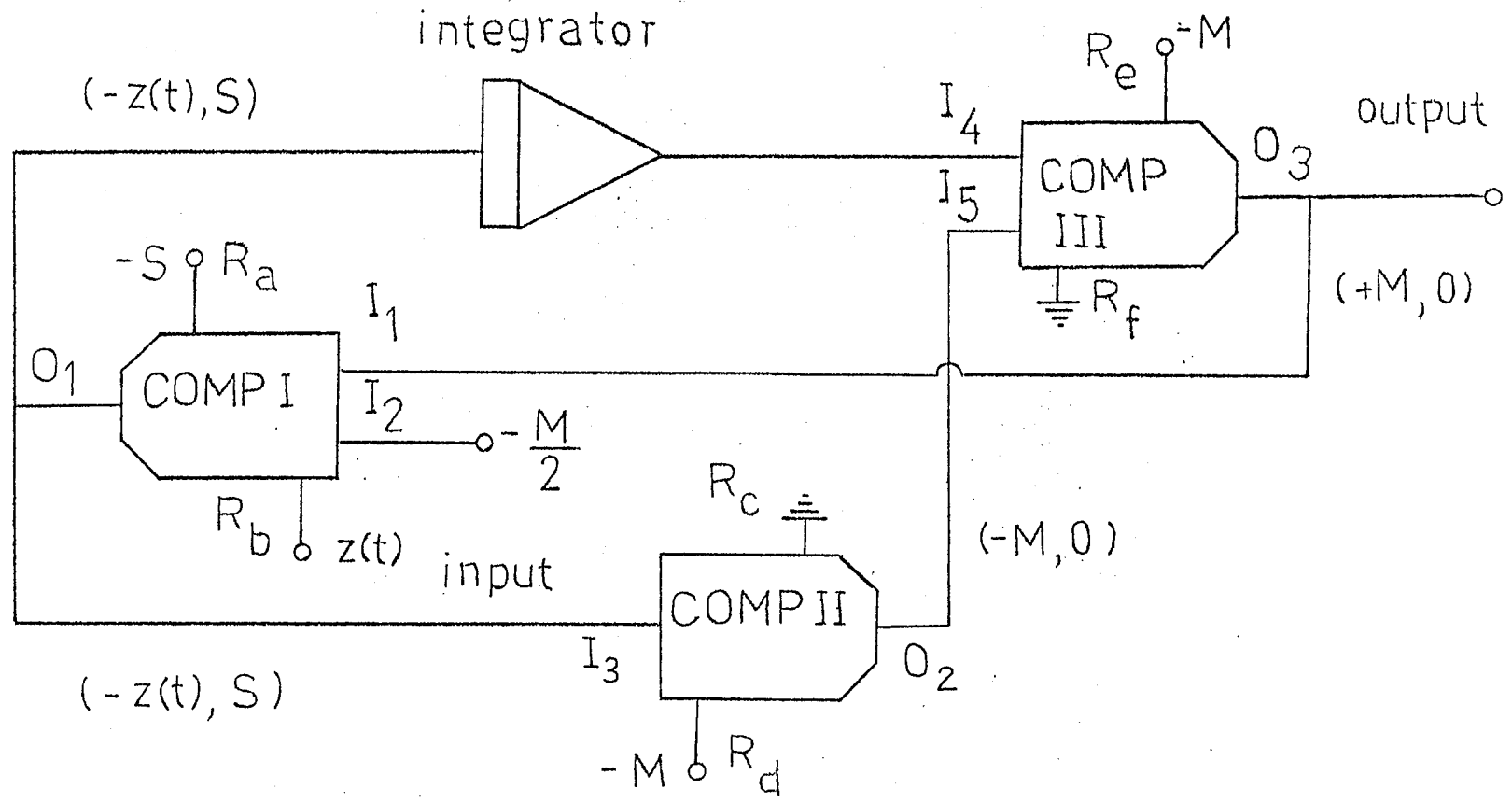


FIGURE 2.21 schematic diagram of IPFM modulator

vice versa. Hence, the polarity of the emitted pulse from the modulator depends on the reference power supply to the electronic comparators. In Fig. 2.2.1, the configuration is arranged to emit positive pulses.

When the modulator begins operation, the reference signal of the three electronic comparators are as shown in Fig. 2.2.1. With the only exception of I_2 , which is at $-M/2$ volts, all the other input legs and output legs for all electronic comparators are zero.

For example, when a positive analog signal, $Z(t)$, is applied to COMP I at R_B , the sum of I_1 and I_2 is negative and $-Z(t)$ is produced at O_1 . The $-Z(t)$ is fed into COMP II and into the integrator. For COMP II, the negative I_3 results in $-M$ volts at O_2 . This $-M$ volts is then fed into COMP III at I_5 . At the same time, the output of the integrator is also fed into COMP III at I_4 , and its value is increasing. The sum of I_5 and I_4 is negative, and O_3 is zero, (i.e. the output of the modulator is zero).

Eventually, the output of the integrator comes to the value which is slightly greater than $+M$ volts. The sum of I_5 and I_4 becomes positive, resulting in $+M$ volts at O_3 . The output of the modulator is now at $+M$ volts.

This $+M$ volts is also fed back to COMP I at I_1 . The sum of I_1 and I_2 becomes positive, and $+S$ volts is then switched to O_1 . The $+S$ volts, which replace $-Z(t)$, is fed into COMP II and into the integrator. For COMP II, the positive I_3 gives zero output at O_2 and hence, at I_5 . The integrator, which is at an instantaneous $+M$ volts output value, is then discharging its potential. There is $+M$ volts at O_3 as long as the sum of I_5 and I_4 is positive. As soon as the sum of

I_4 and I_5 becomes negative, then O_3 is reduced to zero. The output of the modulator becomes zero again, and a standard pulse has been initiated.

This modulation scheme gives a series of pulses with variable spacing for the positive signal, $Z(t)$ (Fig. 2.2.2). These pulses are rectangular in shape at a magnitude of M volts and a duration of Δ seconds. This duration is obtained by calculating the reciprocal of the positive reference power supply S of COMP I. There is no overlapping of pulses with this circuit arrangement because the integration of the incoming analog signal always starts at the termination of the previous pulse.

2.2. Analog Phase Comparator

The simulation of the analog phase comparator is simplified by using a S/360 continuous system modeling program (S/360 CSMP). The S/360 CSMP is a problem-oriented program designed to facilitate the digital simulation of continuous processes on large-scale digital machines. The program includes a basic set of functional blocks that may be used to represent the components of a continuous system. This program also accepts application-oriented statements for defining the connections between these functional blocks.

The block diagram of the analog phase comparator is given in Fig. 2.3.1. It comprises of two resettable flip flop's (i.e. FFI and FFII), an integrator, two zero-order hold devices (i.e. ZHOLD I and ZHOLD II), a multiplier, an inverter and an adder. A resettable flip flop is an electronic logic device in which its output depends on the conditions of its input and its previous output. Its truth table is also given in Fig. 2.3.1. A zero-order hold device is also an electronic logic circuit in which its output depends on the polarity of the controlling signal to the device: a

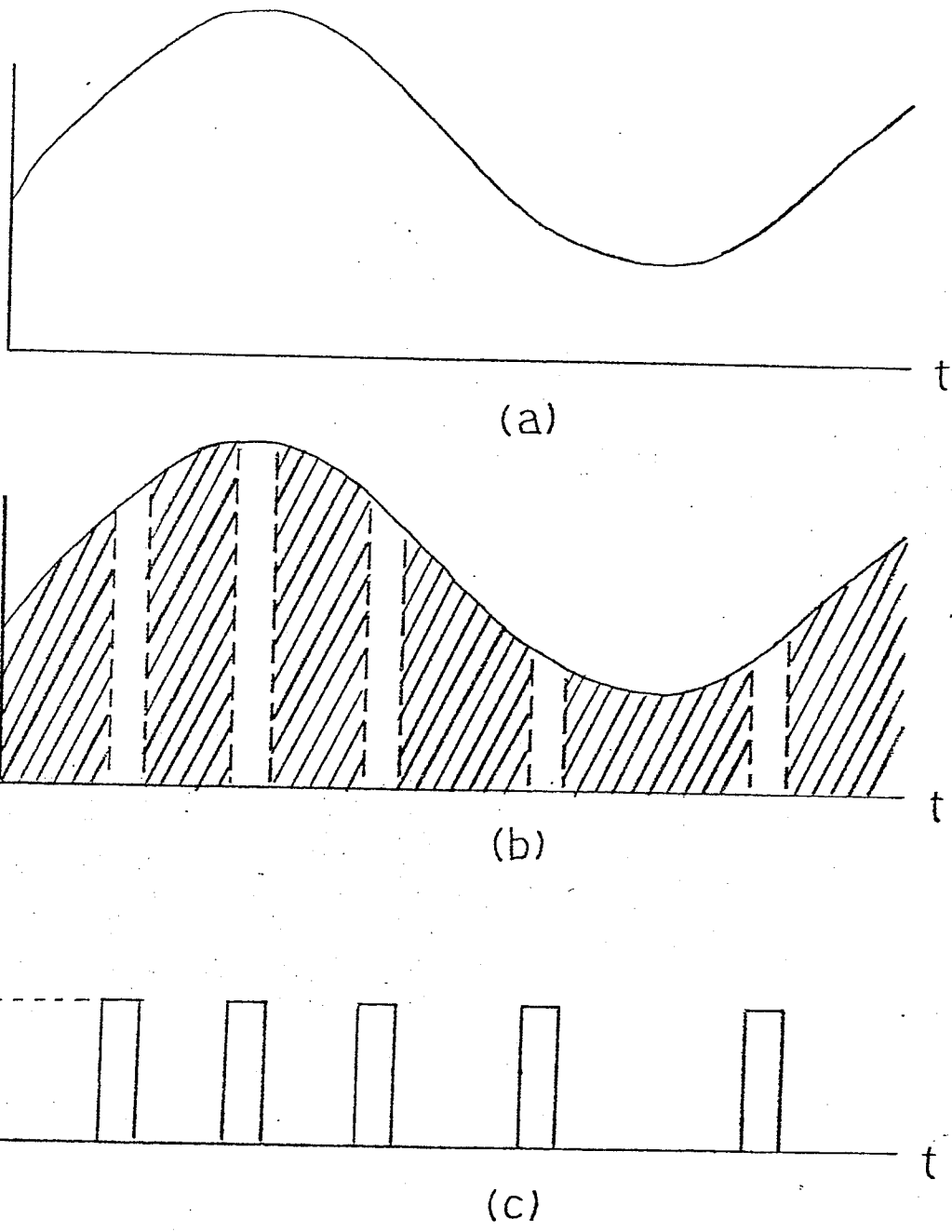
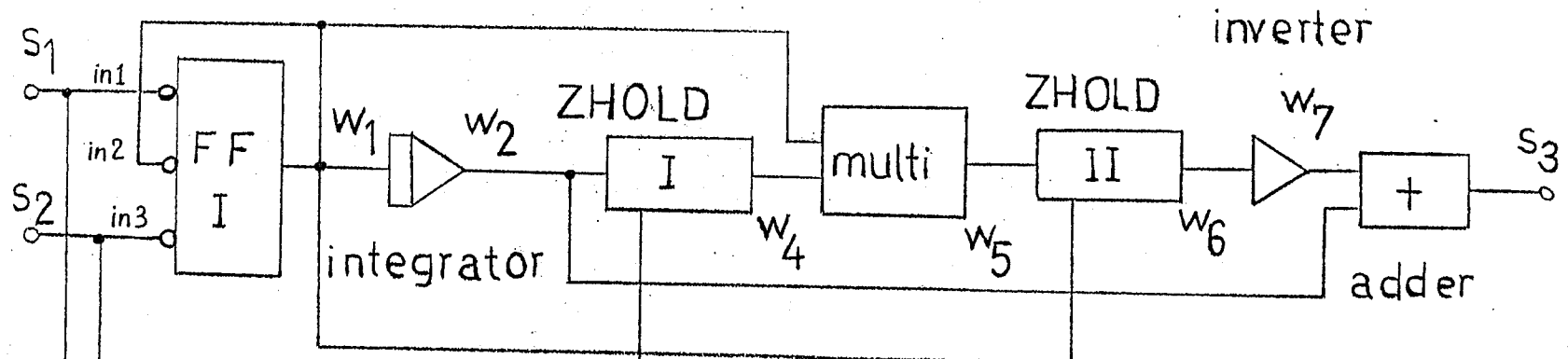


FIGURE 2.2.2
(a) arbitrary input
(b) integrated area (shaded)
(c) IPFM pulses



RST flip flop

out	in1	in2	in3	pre. out
0	+			
1	-	+		
0	-	-	+	1
1	-	-	-	0

truth table of FFI/II

FIGURE 2.3.1 schematic diagram of analog phase comparator

positive controlling signal yields an output which is equal to the input, and a negative or zero controlling signal gives an output which is equal to the previous output.

In Fig. 2.3.1., the system input pulses and the plant output pulses are fed into the analog phase comparator at S_1 and S_2 , respectively. The plant excitation signal appears at S_3 .

When a pulse first comes in at S_1 , FFII is at logic 0 and FFI is at logic 1. The external circuit arrangements of both flip flop's result in zero at W_3 and 1.0 volts at W_1 . The output of ZHOLD I just prior to the appearance of the pulse at S_1 is zero. With no controlling signal at W_3 , the output of ZHOLD I is equal to the previous output and is zero at W_4 . W_1 is fed into the multiplier, ZHOLD II, and the integrator at the same instant. The multiplier multiplies both its inputs at W_4 and W_1 , and, hence, produces zero output at W_5 . Since ZHOLD II now has a positive controlling signal at W_1 , its output at W_6 is now equal to its input at W_5 . W_6 and, hence, W_7 is zero.

The integrator integrates W_1 and generates a unit ramp signal at W_2 . W_2 is fed into ZHOLD I and into an adder, simultaneously. W_2 has no effect on ZHOLD I because there is no controlling signal at W_3 . However, W_2 being fed into the adder, results in a unit ramp signal increasing at a rate of 1.0 volt per sec. at S_3 . The output of the analog phase comparator is a unit ramp signal.

The process is interrupted when another pulse appears at S_2 . FFI is now changed to logic 0 and FFII is changed to logic 1. These changes result in 1.0 volt at W_3 and no signal at W_1 . The controlling signal W_1 to ZHOLD I is then positive so that W_4 is equal to W_2 . The multiplier,

however, yields a zero output at W_5 because there is no input from W_1 . Consequently, W_6 , and then W_7 , are also zero.

Without any input, the integrator maintains a constant output at the level which is the highest integrated value just prior to the change of logic at the flip flop's. The adder compares W_2 from the integrator and W_7 from the inverter, and produces a constant output at S_3 . The output of the analog phase comparator is now constantly at the level which is that of the highest ramp signal, just prior to the appearance of the pulse at S_2 .

When another pulse appears at S_1 , FFI is converted back to logic 1 and FFII to logic 0. These changes result in zero at W_3 and 1.0 volt at W_1 . Without any controlling signal at W_3 , ZHOLD I maintains the constant voltage which is the output of the integrator just prior to the appearance of this pulse. At the multiplier, W_4 multiplies with W_1 , which is 1.0 volt at the moment, and, hence, W_5 is equal to W_4 . ZHOLD II is at a positive 1.0 volt controlling signal, and W_6 is equal to W_5 . The inverter changes the sign of W_6 and W_7 is equal to $-W_4$.

Simultaneously, the integrator starts integrating W_1 and produces another ramp signal at W_2 . ZHOLD I blocks this ramp signal at W_2 because there is no signal at the controlling point W_3 . W_2 is, however, compared with W_7 at the adder. Hence, the analog phase comparator is reset to zero before it produces another ramp signal. Hence, the output signal of the analog phase comparator is a sequence of trapezoidal signals(Fig. 2.3.2).

The integrator always integrates between any input pulse and the immediately following feedback pulse. These intervals provide the ramp portion of the trapezoidal signal. The output of the phase comparator remains constant between any feedback pulse and the immediately succeeding

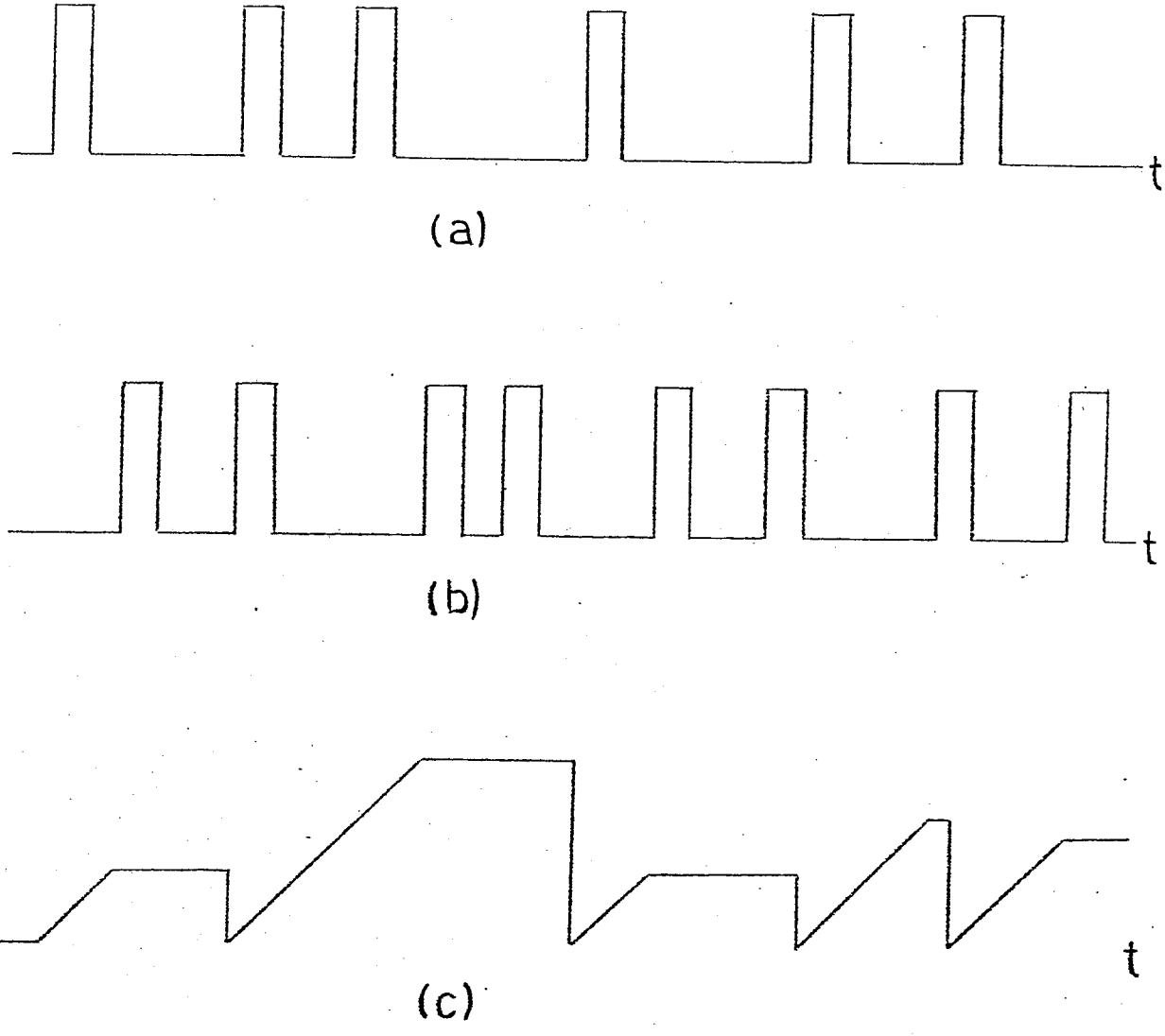


FIGURE 2.3.2
(a) input IPFM pulses
(b) feedback IPFM pulses
(c) analog phase comparator output

input pulse. All these intervals produce the flat portion of the trapezoidal signal.

The duration of every individual trapezoid depends on the duration of every input-feedback-input pulse trio. The closer the feedback pulse is to the preceding input pulse, the shorter is the duration of the ramp portion of the trapezoid; resulting in a small magnitude of the trapezoid. On the other hand, the farther away the feedback pulse is from the preceding input pulse, the longer is the duration of the ramp portion of the trapezoid. This increases the magnitude of the trapezoid.

CHAPTER 3

ANALYSIS OF LOCKING CONDITIONS

Since related analyses have not been done previously, the locking conditions of phase-locked systems are investigated in this Chapter. The objective is to study the system performance for different values of plant gain and for different system parameters. The approach taken is to simulate different systems on a digital computer in order to gain insight into the system behaviour. This insight is then used in developing the theoretical locking conditions.

3.1. Simulation of Phase-Locked Systems

Continuous System Modelling Program (CSMP) is used to simulate the phase-locked systems on a digital computer. These simulated systems are regulator systems (i.e. systems with constant input) whose inputs are fed into an Integral Pulse Frequency Modulator to produce a train of rectangular pulses at constant intervals. Various systems are simulated to obtain some insight of the system behaviour.

In the following simulations, all the system parameters are standardized so as to compare the different system performances on the same scale. Since it is very difficult to simulate impulses for this particular purpose in the CSMP, the two IPFM modulators are designed to emit rectangular pulses with 1.0 volt in magnitude and 0.05 seconds in duration. The 1.0 volt is chosen arbitrarily and the 0.05 sec is the time at which this IPFM scheme requires to reset the integrator. The predetermined threshold levels for the IPFM modulators are simply selected to be 1.0 volt-second. For ease of observations on the computer printout, the system input is purposely designed

at 1.0526315 volts, so that while the first input pulse is initiated at 0.975 seconds, the remaining input pulses are exactly at 1.0-second intervals. The trapezoidal signals from the analog phase comparator are designed to have their ramp portions climbing at a rate of 1.0 volt per second. The following responses are based on these standardized system parameters.

A first-order linear plant with its pole location at -1.0 is chosen to be simulated. Different plant gain values are assigned to the system. It is observed that the system is phase-locked for only a certain region of gain. Among them, the gain of 2.2, 2.7 and 3.85 provides fairly satisfactory results (Fig. 3.1.1, 3.1.2 and 3.1.3). The system does not phase-lock if the plant gain is assigned below or above this region.

At a gain of 2.2, the feedback pulses are locked to the input pulses in 3.975 seconds, three seconds after the first pulse appears, even though the feedback pulses are slightly oscillating around the input pulses. At 12.975 seconds, nine seconds later, the feedback pulses become stable and are initiated at constant inter-pulse intervals of 0.85 seconds. The plant output becomes regular and periodic. The maximum is 1.26 volt at the initiations of input pulses and the minimum is 0.96 volts at 0.425 seconds later from each input pulse (Fig. 3.1.1).

At a gain of 2.7, the system also requires three seconds to achieve phase-locked states. After another six seconds later, the feedback pulses are initiated regularly at a constant inter-pulse interval of 0.5 seconds. After the system is phase-locked and stable, the plant output becomes regular and periodic. The plant output has a maximum of 1.175 volts at the initiation of each input pulse and a minimum of 0.945 volts at 0.25 seconds later (Fig. 3.1.2).

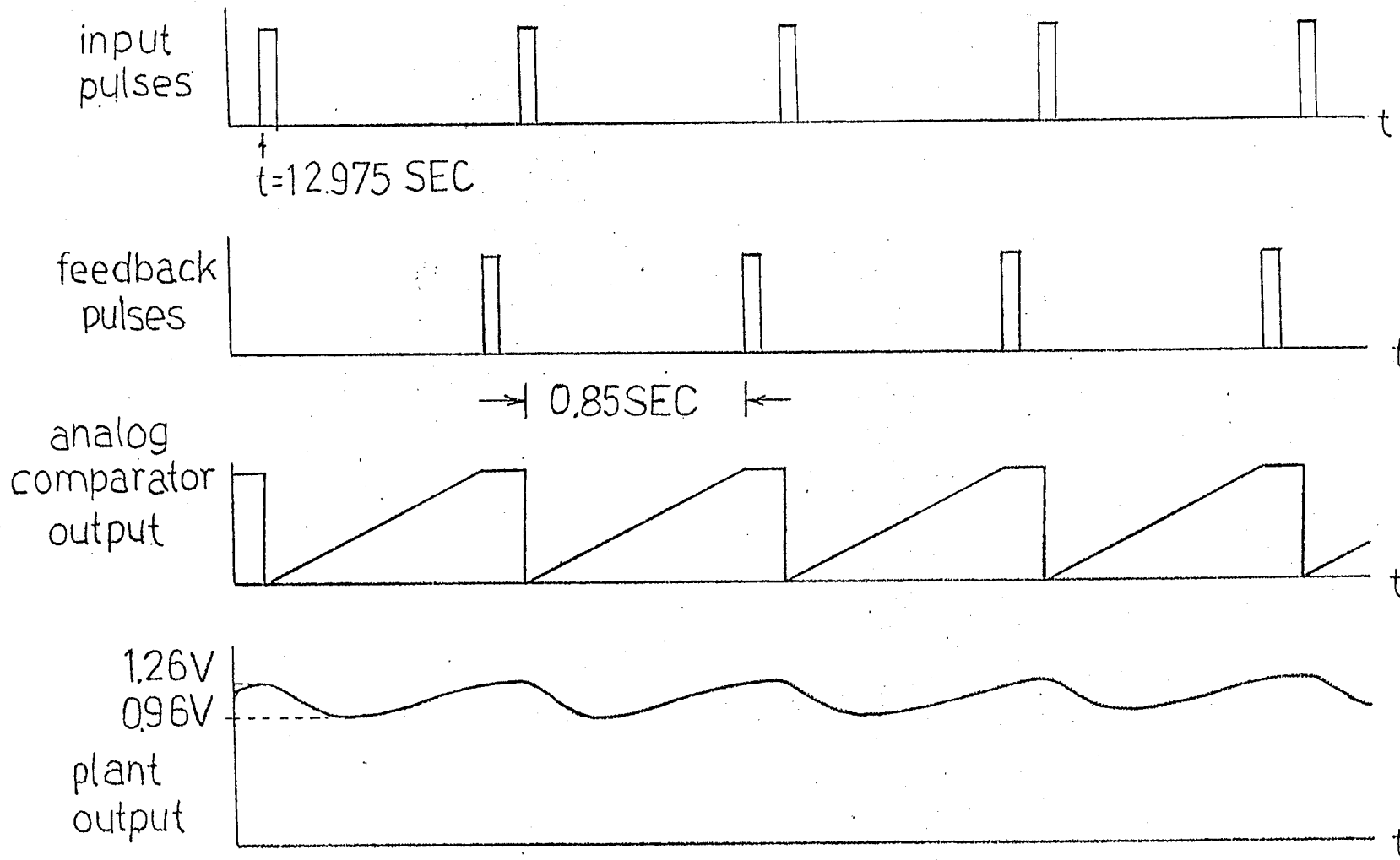


FIGURE 3.1.1. system behaviour (pole at -1, gain at 2.2)

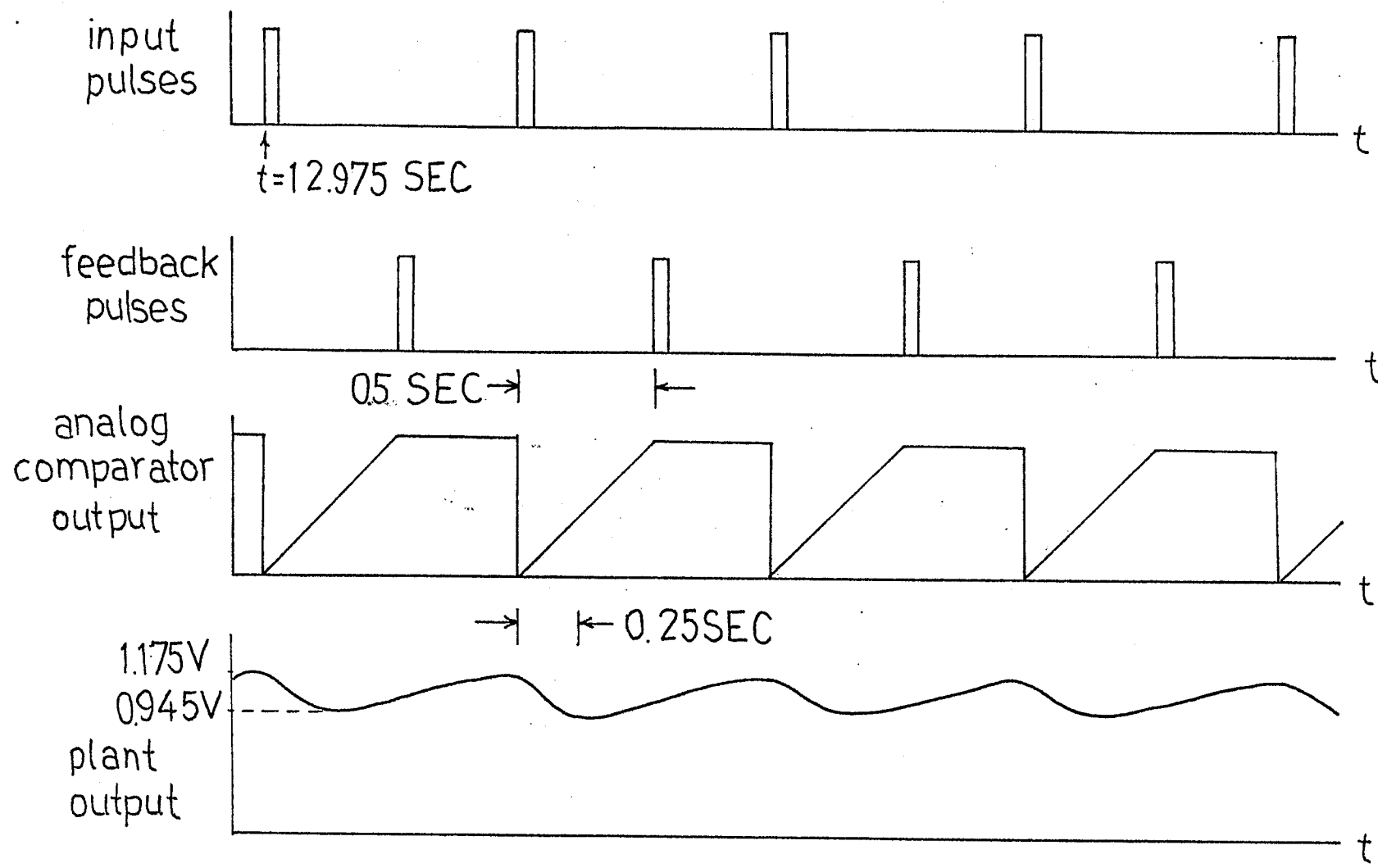


FIGURE 3.1.2 system behaviour (pole at -1, gain at 2.7)

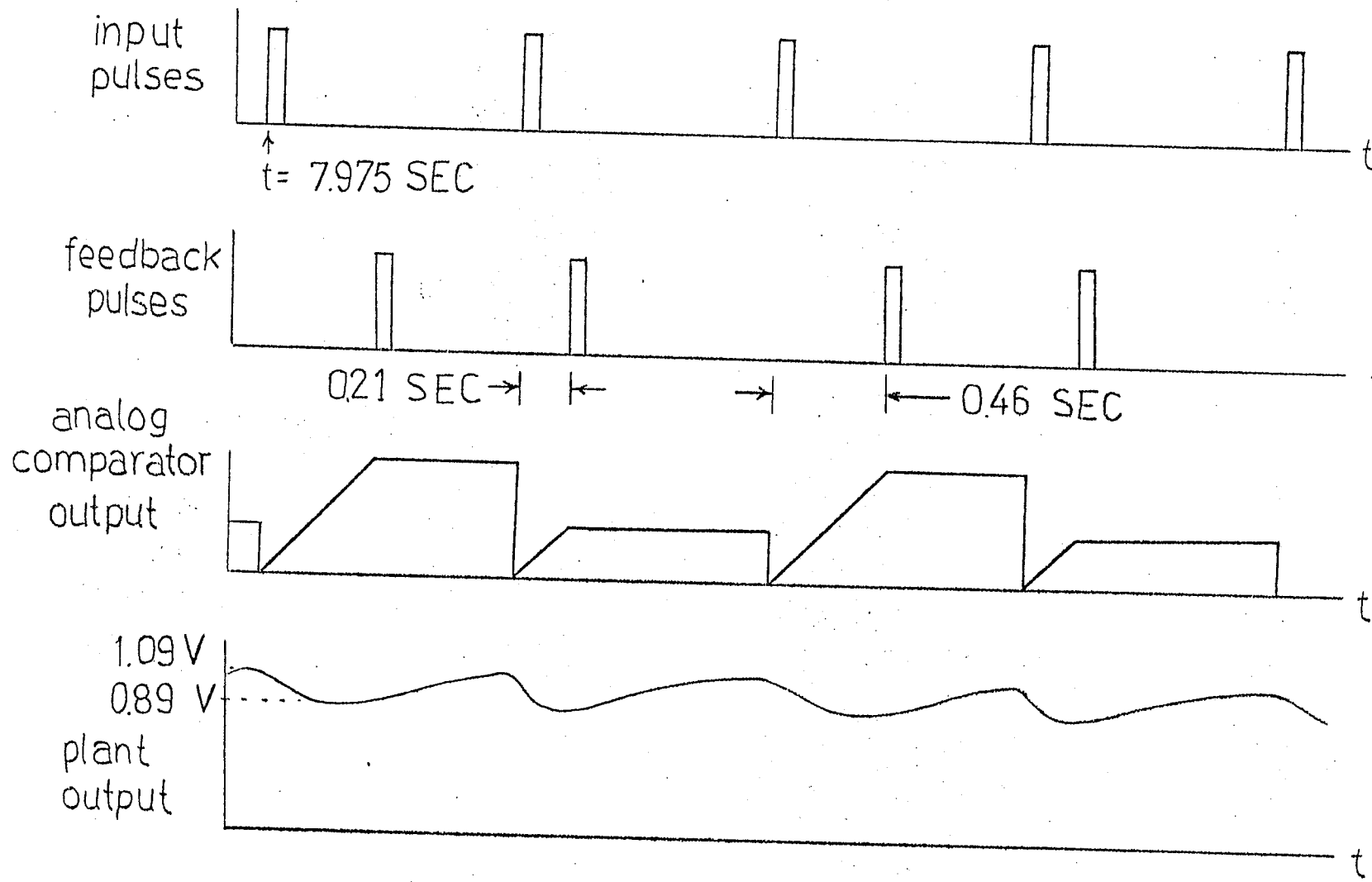


FIGURE 3.1.3 system behaviour (pole at -1, gain at 3.85)

The system is then assigned a gain of 3.85. It requires three seconds to achieve phase-lock. A peculiar initiation pattern of the feedback pulses occurs at another four seconds later. Since then, the feedback pulses are initiated at the inter-pulse interval of either 0.2125 seconds or 0.4625 seconds. Even though the system is still phase-locked (Fig. 3.1.3), the feedback pulses are not stable at this gain; i.e., they are oscillating around the input pulses.

From these observations, the system is phase-locked when appropriate plant gain is applied to the system. There are apparently minimum and maximum limits of plant gain for each system. It would not be able to lock if the plant gain is below the minimum limit; the feedback IPFM modulator does not have sufficient input so that it can initiate pulses at the required time slots. Also, from the observation, high plant gain may create oscillation and force the system out of lock. Hence, analysis of locking conditions is simplified to the determination of appropriate plant gain for particular systems.

3.2. Locking Conditions

In order to analyze the locking conditions of the system, a general expression of the plant output $y(t)$ is established for systems with different order linear plants. Since the plant output $y(t)$ in Fig. 3.2.1 is periodic with a period equal to that of the input pulses, the value of the integral of $y(t)$, for any pulse interval (i.e., $t_K \leq t \leq t_{K+1}$), is evaluated in order to find the relationship of the plant gain K with other system parameters. With this relationship, the conditions for phase-locking are obtained.

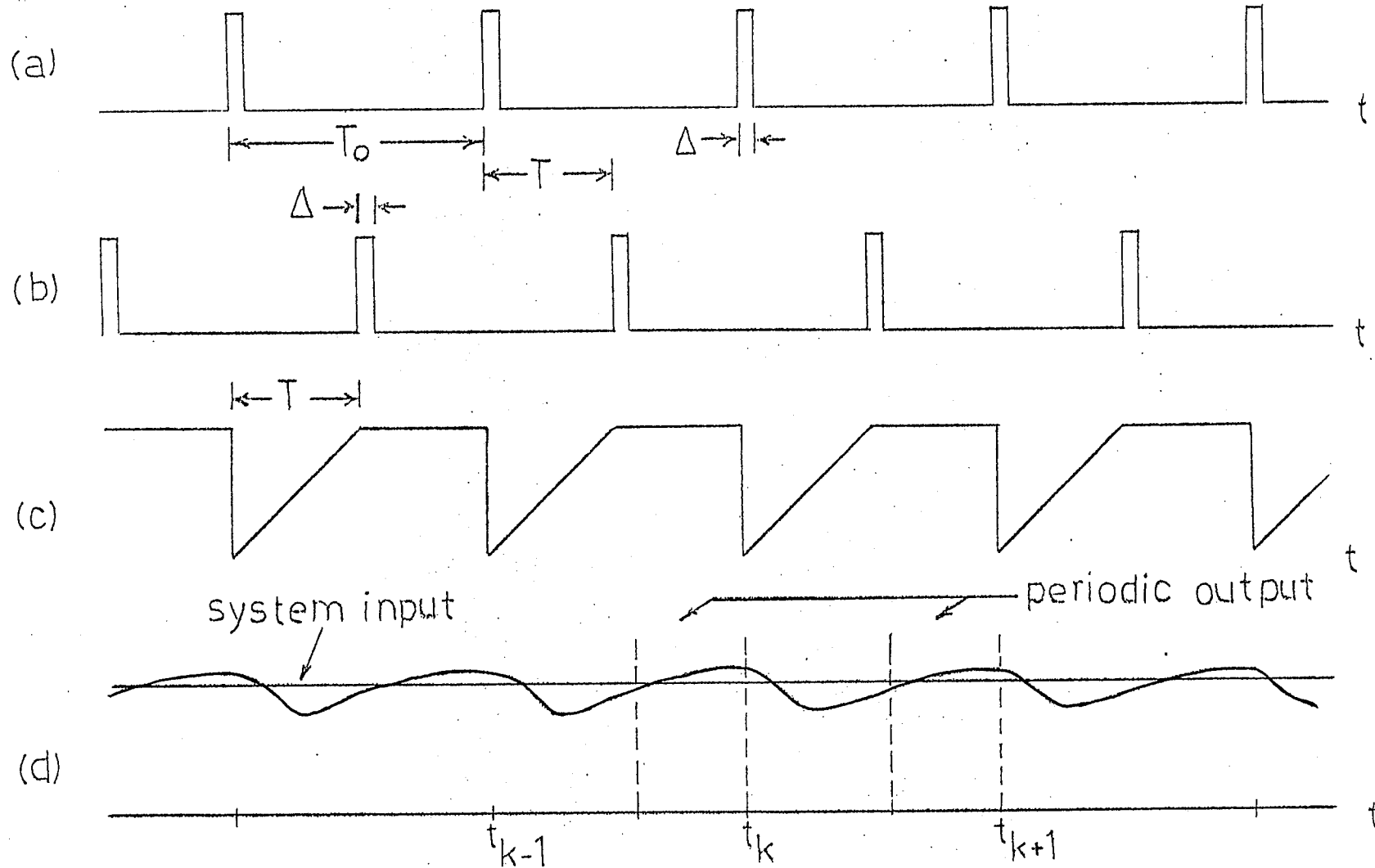


FIGURE 3.2.1 (a) input pulses, (b) feedback pulses, (c) comparator output, $x(t)$, (d) plant output, $y(t)$, and system input

Consider the linear plant which is represented by the following nth order linear differential equation,

$$y(t)^{(n)} + f_1 y(t)^{(n-1)} + f_2 y(t)^{(n-2)} + \dots + f_n y(t) = K x(t) \Big|_{t \geq t_r} \quad (3.1)$$

where t_r is the reference time at which the first input pulse is initiated and f_i 's are constants.

The nth order differential equation can be transformed into a set of first order differential equations; namely,

$$\begin{aligned} \dot{y}_1(t) + a_1 y_1(t) &= y_2(t) \\ \dot{y}_2(t) + a_2 y_2(t) &= y_3(t) \\ \vdots \\ \dot{y}_n(t) + a_n y_n(t) &= K X(t) \end{aligned} \Big|_{t \geq t_r}$$

or, in matrix form,

$$\underline{\dot{Y}}(t - t_r) = \underline{A} \underline{Y}(t - t_r) + \underline{Q} X(t - t_r) \quad (3.2)$$

Where

$$\underline{A} = \begin{bmatrix} -a_1 & 1 & 0 & & \\ 0 & -a_2 & 1 & 0 & \\ \vdots & & & & \\ 0 & & & 0 - a_n & \end{bmatrix} \text{ and } \underline{Q} = \begin{bmatrix} 0 \\ 0 \\ \vdots \\ K \end{bmatrix}$$

The general form of the solution to Eq. (3.2) is obtained by the following equation

$$\underline{Y}(t - t_r) = e^{\underline{A}(t-t_r)} \underline{C} + \int_{t_r}^t e^{\underline{A}(t-v)} \underline{Q} \underline{X}(v - t_r) dv \quad (3.3)$$

where \underline{C} is a constant matrix depending on initial conditions. Hence, the state, $\underline{Y}(t - t_r)$, for $t \geq t_r$ is uniquely determined by the state at time t_r and the input for $t \geq t_r$, and it is independent of the state and the input before t_r .

In the following, the analysis is based on the assumption that, in steady state, the control system is phase-locked and stable so that the feedback pulses are initiated at constant inter-pulse intervals (Fig. 3.2.1(a), and (b)). Also, the signals exciting the plant become a train of identical trapezoids (Fig. 3.2.1(c)). Since $\underline{Y}(t - t_r)$ is continuous and periodic (Fig. 3.2.1(d)), it is only required to obtain mathematical description of $\underline{Y}(t - t_r)$ between t_K and t_{K+1} . In Fig. 3.2.1, t_K is chosen as the new reference time and Eq. (3.3) becomes

$$\underline{Y}(t - t_K) = e^{\underline{A}(t - t_K)} \underline{Y}_{t_K} + \int_{t_K}^t e^{\underline{A}(t - v)} \underline{Q} \underline{X}(v - t_K) dv \quad (3.4)$$

where \underline{Y}_{t_K} is the state of the control system at t_K . For $t_K \leq t \leq t_K + T$ where T is the inter-pulse interval, $\underline{X}(t - t_K) = t - t_K$ and for $t_K \leq t \leq t_K + T_0$, where T_0 is the input pulse period, $\underline{X}(t - t_K) = T$.

$$\begin{aligned} \underline{Y}(t - t_K) &= (e^{\underline{A}(t - t_K)} \underline{Y}_{t_K} - (t - t_K) \underline{A}^{-1} \underline{Q} + \underline{A}^{-2} e^{\underline{A}(t - t_K)} \underline{Q} - \underline{A}^{-2} \underline{Q}) u(t - t_K) \\ &\quad + (\underline{A}^{-1} (t - t_K - T) - \underline{A}^{-2} e^{\underline{A}(t - t_K - T)} \underline{Q} + \underline{A}^{-2} \underline{Q}) u(t - t_K - T) \end{aligned} \quad (3.5)$$

where $u(t)$ is a unit step function.

It is required to determine \underline{Y}_{t_K} . At $t = t_K + T_o$, Eq. (3.5) becomes

$$\underline{Y}(t_K + T_o - t_K) = e^{\frac{AT}{o}} \underline{Y}_{t_K} - \underline{TA}^{-1} \underline{Q} + \underline{A}^{-2} (e^{\frac{AT}{o}} - e^{\frac{A(T_o - T)}{}}) \underline{Q}$$

(3.6)

From Fig. 3.2.1(d), $\underline{Y}_{t_K} = \underline{Y}_{t_{K+1}} = \underline{Y}(T_o)$. Substitute into Eq. (3.6) and get

$$\underline{Y}_{t_K} = (\underline{I} - e^{\frac{AT}{o}})^{-1} \underline{A}^{-2} (e^{\frac{AT}{o}} - \underline{A}^T - e^{\frac{A(T_o - T)}{}}) \underline{Q}$$

(3.7)

The plant output, $\underline{Y}_1(t)$ (or $y(t)$), is of prime interest. $\underline{Y}_1(t)$ can be obtained by defining a known matrix \underline{H} , where

$$\underline{H} = [1 \quad 0 \quad 0 \quad \dots \quad 0]$$

From Eq. (3.5),

$$\begin{aligned} \underline{y}_1(t-t_K) &= \underline{H} (e^{\frac{A(t-t_K)}{}}) \underline{Y}_{t_K} - (t-t_K) \underline{A}^{-1} \underline{Q} + \underline{A}^{-2} e^{\frac{A(t-t_K)}{}} \underline{Q} - \underline{A}^{-2} \underline{Q} u(t-t_K) \\ &\quad + \underline{H} (\underline{A}^{-1} (t-t_K - T) - \underline{A}^{-2} e^{\frac{A(t-t_K-T)}{}} \underline{A} + \underline{A}^{-2} \underline{Q}) u(t-t_K-T) \end{aligned}$$

(3.8)

From Eq. (3.6),

$$\underline{y}_1(t_K) = \frac{-T \underline{H} \underline{A}^{-1} \underline{Q} + \underline{H} \underline{A}^{-2} (e^{\frac{AT}{o}} - e^{\frac{A(T_o - T)}{}}) \underline{Q}}{1 - u_{11}(T_o)}$$

(3.9)

where

$$[u_{ik}(T_o)]_{nxn} = e^{\frac{AT}{o}}$$

In Fig. 3.2.1(d), the feedback IPFM, which starts integrating the

plant output $y_1(t)$ at $t_{K-1} + T + \Delta$, emits a standard pulse at $t_K + T$, and the integral of the plant output $y_1(t)$ in this interval equals the threshold level E of the modulator. Since the plant output $y_1(t)$ is continuous and periodic, the plant output $y_1(t)$ between $t_{K-1} + T + \Delta$ and t_K would be identical to that between $t_K + T + \Delta$ and t_{K+1} . Assuming the pulse duration Δ to be negligible,

$$E = \int_{t_K}^{t_K + T_0} y_1(t) dt \quad (3.10)$$

Also, the plant gain K is an explicit parameter of the expression $y_1(t)$, and Eq. (3.10) becomes

$$E = K L(T) \quad (3.11)$$

where

$$L(T) = \frac{1}{K} \int_{t_K}^{t_K + T_0} y_1(t) dt$$

Hence, the plant gain K is related to the inter-pulse interval T by Eq. (3.11). A plot relating the gain K and the inter-pulse interval T for first order systems with different pole positions is shown in Fig. 3.2.2. For locking, the inter-pulse interval T can be any positive value, provided that it is less than the input pulse period T_0 . If the inter-pulse interval T is assumed to be greater than T_0 , there will be no feedback pulse in the specific time slot, and the system will not be phase-locked. It is shown in Fig. 3.2.2 that as the plant gain K increases the inter-pulse interval T becomes smaller. Intuitively, higher plant gain creates large system output so that the feedback pulses are initiated sooner. The gain K in the lower

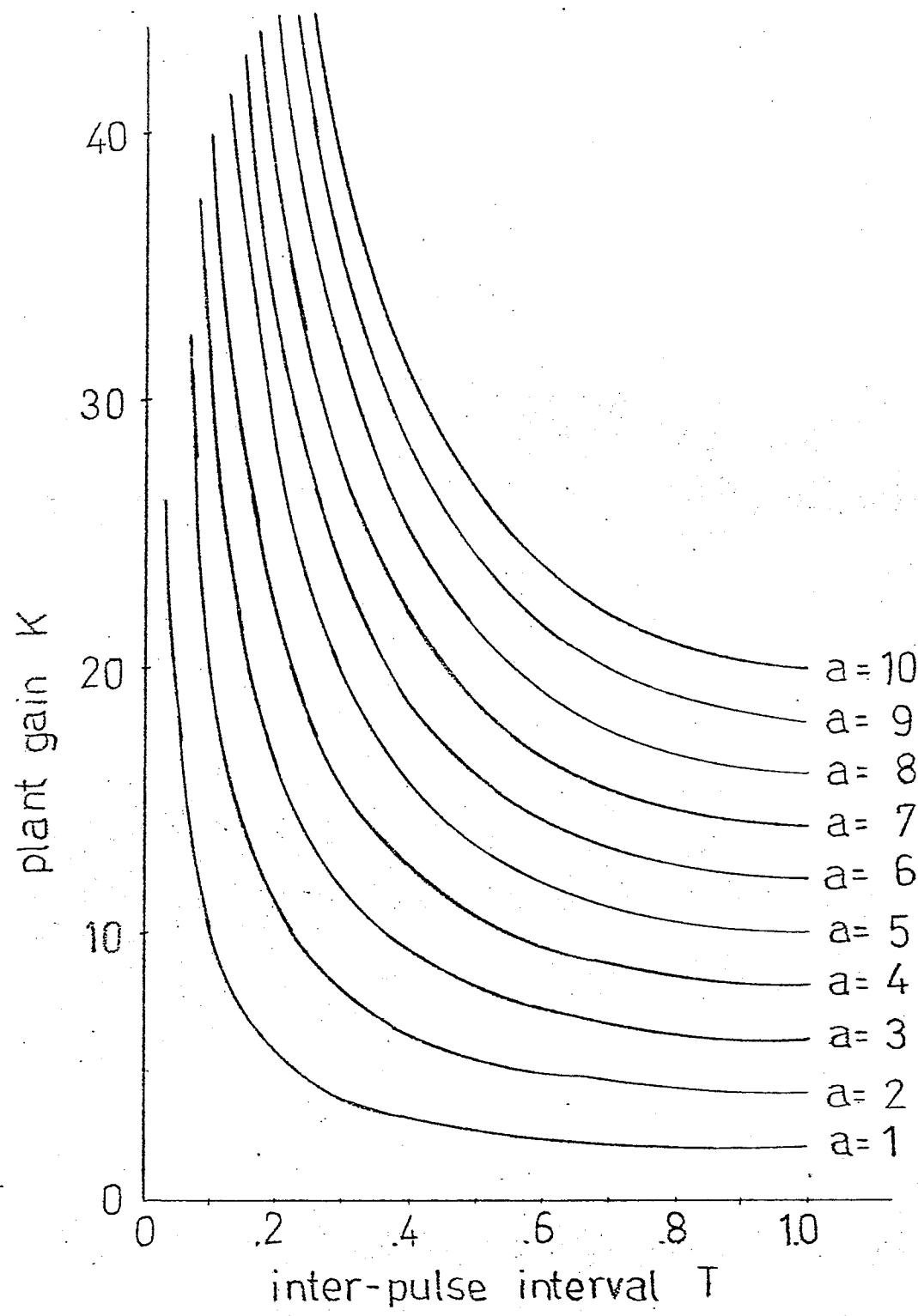


FIGURE 3.2.2 plant gain for locking
(1st order systems)

region coincides with the observation in Section 3.1. However, when the plant gain is increased to the point where T is at about 0.3 seconds, then the feedback pulse positions are observed to oscillate; that is, it is observed that the steady state solution becomes unstable. Hence, it is necessary to investigate stability.

CHAPTER 4

STABILITY

When system simulations were done to verify the locking conditions, it was observed that the feedback pulse positions oscillated around the 'theoretical value' as the plant gain was increased. Further increases in plant gain caused the plant to come out of 'lock'. Because the steady state solution was observed to be unstable it became necessary to investigate the stability of a phase-locked system.

4.1. Stability of a Phase-Locked System

As already pointed out, the feedback pulse position oscillates around the calculated values as the gain is increased. Intuitively, it can be seen that if a feedback pulse occurs too late, the signal exciting the plant and the corresponding plant output will be large. Consequently, the next feedback pulse will occur too soon and the signal exciting the plant will be small. This results in a late occurrence of the next pulse. The situation keeps on repeatedly and the feedback pulses will not be able to settle down to the calculated values.

In the case where the feedback pulses are oscillating in the neighbourhood of the 'theoretical' position, the actual plant input signal (solid line in Fig. 4.1.1(a)) is

$$X(t) = X_T(t) + X_d(t) \quad (4.1)$$

where $X_d(t)$ is the deviation of the actual plant input signal from the plant input signal under periodic conditions $X_T(t)$.

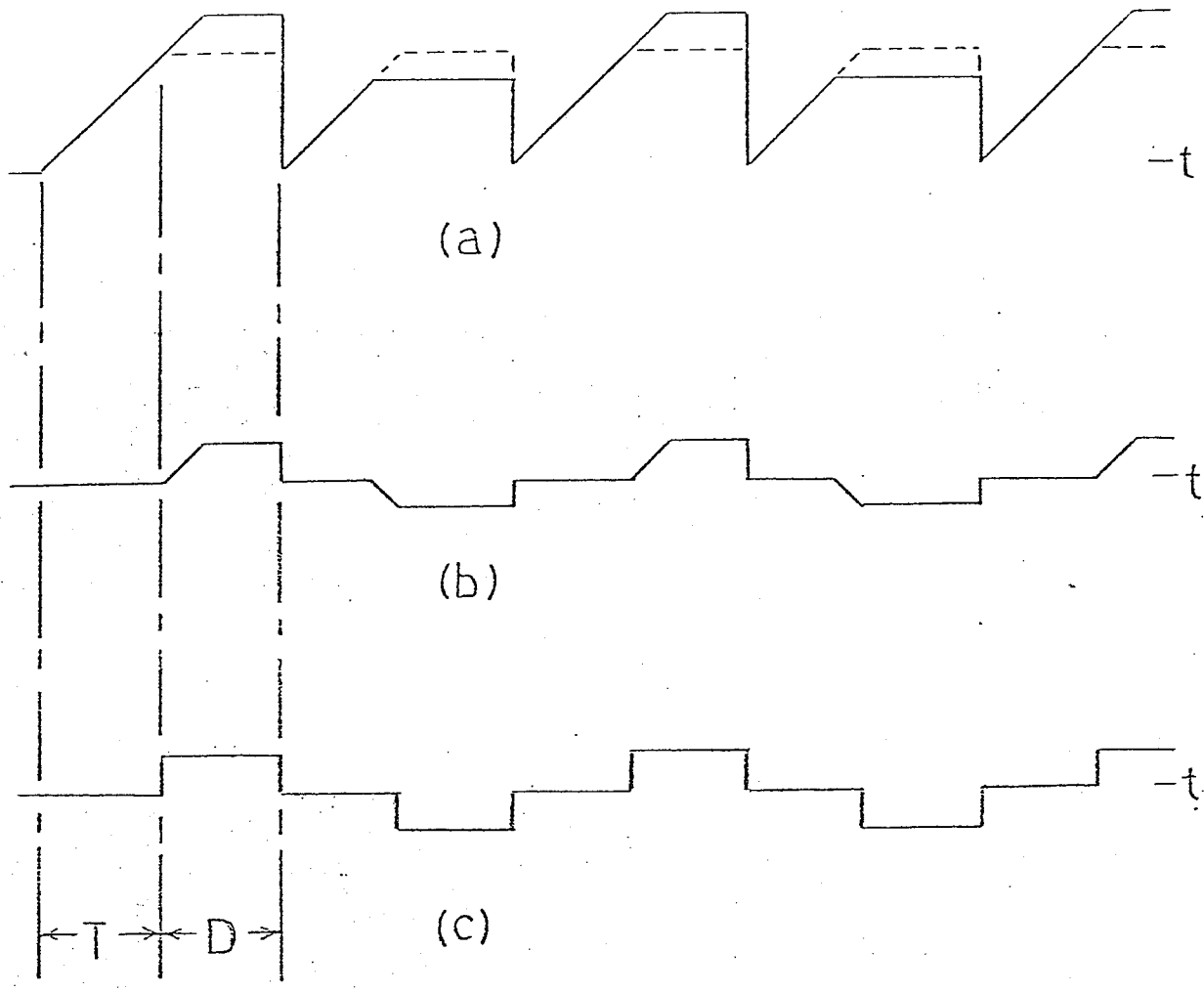


FIGURE 4.11 (a) $X(t) = X_T(t) + X_d(t)$
(b) $X_d(t)$
(c) approximated square wave

The signal $X_d(t)$ is assumed to have small average amplitude as compared to $X_T(t)$. Hence, $X_d(t)$ is a sequence of positive and negative trapezoidal signals (Fig. 4.1.1(b)). Since $X_d(t)$ is assumed small and deviates from $X_T(t)$ in a specific pattern, $X_d(t)$ can be approximated by a sequence of alternating square waves (Fig. 4.1.1(c)).

Studying the stability of the periodic solution defined by $X(\bar{t}) = X_T(t)$ is equivalent to studying the behaviour of $X_d(t)$ when $X_d(t)$ is fed into the linear plant of the system with the loop closed⁽¹⁾. More precisely, the stability of a phase-locked system is the same as the stability of a sampled-data control system with a hold device which holds the signal value for D seconds (Fig. 4.1.2).

Under such conditions, stability can be investigated by applying the technique of the sampled-data control theory to the sampled-function locus

$$K G(z) = K \mathcal{Z} \left[\left(\frac{1 - e^{-DS}}{S} \right) G(s) \right] \quad (4.2)$$

where the transport lag D is smaller than the sampling period T_o . Instability will occur if the Nyquist Locus $KG^*(j\omega)$ encircles the critical point -1 . Stability will occur if the Nyquist Locus $KG^*(j\omega)$ does not encircle the -1 point. This will be used to determine the system stability.

4.2. Determination of System Stability

The procedure for finding the system gain, K , for stable PLL

(1) See page 477-480 of "Feedback Control Systems" by Gille, Pelegrin and Decaulne.

sampling period, T_0

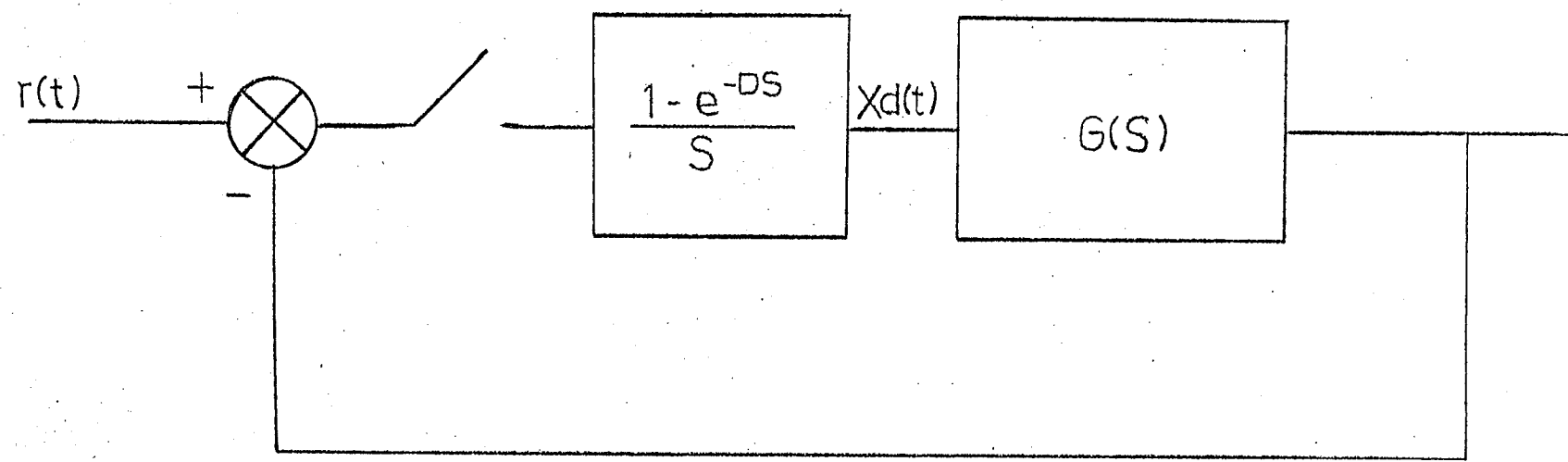


FIGURE 4.1.2 sampled-data feedback control system with special hold device

operation is demonstrated for first and second order systems with real poles. This procedure is applicable to general nth order systems; however, it becomes more cumbersome as the system order increases.

In the previous Chapter, a general expression regarding the locking conditions for systems of nth order linear plants is obtained. For any linear plant with real poles, the poles are either distinct or multiple. In the second order systems, for example, the plants can have either two distinct poles or a multiple pole of order two. The plant gain for which the systems are theoretically phase-locked can be obtained easily by using the Lagrange interpolation formula for systems of second or higher orders (G1).

The concept of sampled-data control systems with a special hold device is applied to the stability of phase-locked systems. In general, the characteristic equation of a sampled-data control system with the special hold device may be derived by putting the denominator of the system output transform as shown in Fig. 4.1.2 equal to zero. The characteristic equation of the system is given by

$$1 + K G (Z) = 0 \quad (4.3)$$

The nature of the roots of Eq. (4.3) determines the stability of the system. The system is stable if all the roots of the characteristic equation in Z lie inside the unit circle about the origin of the Z plane. The gain of stable first order systems for different inter-pulse interval T are plotted in Fig. 4.2.1. It is shown that the gain begins with some small value and increases as the inter-pulse interval T increases.

The locking conditions of a phase-locked system are determined by the steady state solution as given in Eq. (3.11). Eq. (3.11) provides the

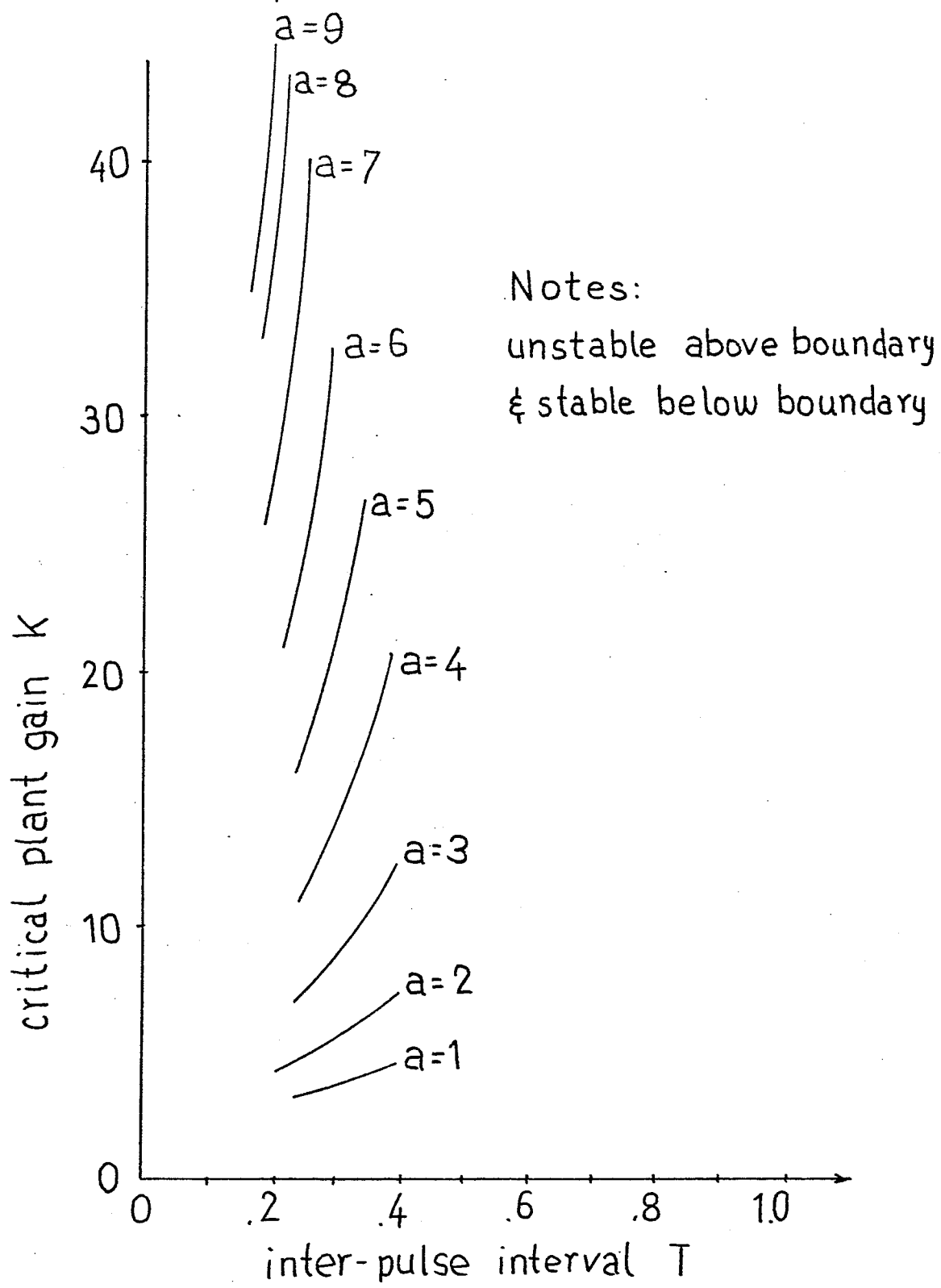


FIGURE 4.21 stability limits for 1st order systems

theoretical region of plant gain K within which the system would be phase-locked but it does not address itself to stability. This expression works well at lower plant gain, but as soon as the plant gain increases, it is not sufficient to predict the oscillation of the feedback pulses. The stability can be determined by the characteristic equation of sampled-data systems with the special hold device as shown in Eq. (4.3). The intersection of the stability limit curve (Eq. (4.3)) and the locking condition curve (Eq. (3.11)) establishes the maximum gain and the minimum inter-pulse intervals for stable operation.

First Order System

In the case of a first order system, the linear plant can be represented by the following differential equation:

$$\dot{y}(t) + a y(t) = K X(t) \Big|_{t \geq t_K} \quad (4.4)$$

Since it is a first order differential equation; then

$$\underline{A} = -a$$

$$\underline{A}^{-1} = -1/a$$

$$\underline{Q} = K$$

$$\underline{H} = 1$$

$$u_{11}(T_o) = e^{-aT_o}$$

From Eq. (3.9)

$$y_{1t_K} = \frac{K(aT_o + e^{-aT_o} - e^{-a(T_o-T)})}{a^2(1 - e^{-aT_o})}$$

From Eq. (3.8), the system output between t_K and t_{K+1} is

$$\begin{aligned}
 y_1(t-t_K) &= \frac{-aT_0 - a(t-t_K)}{a^2(1-e^{-aT_0})e^{-at}} u(t-t_K) \\
 &+ \frac{K(a(t-t_K) + e^{-a(t-t_K)} - 1)}{a^2} u(t-t_K) \\
 &- \frac{K(a(t-T-t_K) + e^{-a(t-T-t_K)} - 1)}{a^2} u(t-t_K-T) \quad (4.5)
 \end{aligned}$$

From Eq. (3.10), the gain of the system with first order linear plant is

$$K = \frac{E}{L}$$

where

$$L = \frac{T(T_0 - T/2)}{a} \quad (4.6)$$

For the system with first order linear plants, the range of plant gain, for which the systems are theoretically phase-locked, depends on the interrelationship of the threshold level, E , of the IPFM modulator and the value of L . The threshold level, E , is a predetermined value and L is a simple expression which includes the pole a , the input pulse period T_0 and the inter-pulse interval T . Since T can be any value between 0 and T_0 , the required gain for locking can be obtained by assigning different values of T to the expression.

The stability of the first order system is determined by means of the Root-locus Method in the Z plane for the first order sampled-data control system with the special hold device. From Eq. (4.2),

$$K G(S) = K \frac{(1 + e^{-DS})}{S(S+a)}$$

The corresponding Z transform is

$$K G(Z) = \frac{K(e^{-aT} - e^{-\frac{aT}{a}})}{a(Z - e^{-\frac{aT}{a}})} \quad (4.7)$$

The characteristic equation is given by

$$1 + K G(Z) = 1 + \frac{K(e^{-aT} - e^{-\frac{aT}{a}})}{a(Z - e^{-\frac{aT}{a}})} \quad (4.8)$$

and

$$Z - e^{-\frac{aT}{a}} + \frac{K(e^{-aT} - e^{-\frac{aT}{a}})}{a} = 0$$

The pole configuration for $G^*(Z)$ and the root locus in the Z plane for the characteristic equation are shown in Fig. 4.2.2.

In view of the fact that the Z transformation maps the left half of the S plane into the interior of the unit circle of the Z plane, absolute stability requires that all poles of the output Z transform lie inside the unit circle. In other words, for stable operation the root locus of this sampled-data system must be confined in the unit circle. The gain at which instability occurs is the plant gain at which the root locus intersects the unit circle, and will be referred to as the critical gain. The point of intersection is located at $-1 + j0$. (Fig. 4.2.2). Hence, from Eq. (4.8)

$$\begin{aligned} -1 - e^{-\frac{aT}{a}} + \frac{K(e^{-aT} - e^{-\frac{aT}{a}})}{a} &= 0 \\ K &= \frac{a(1 + e^{-\frac{aT}{a}})}{(e^{-aT} - e^{-\frac{aT}{a}})} \end{aligned} \quad (4.9)$$

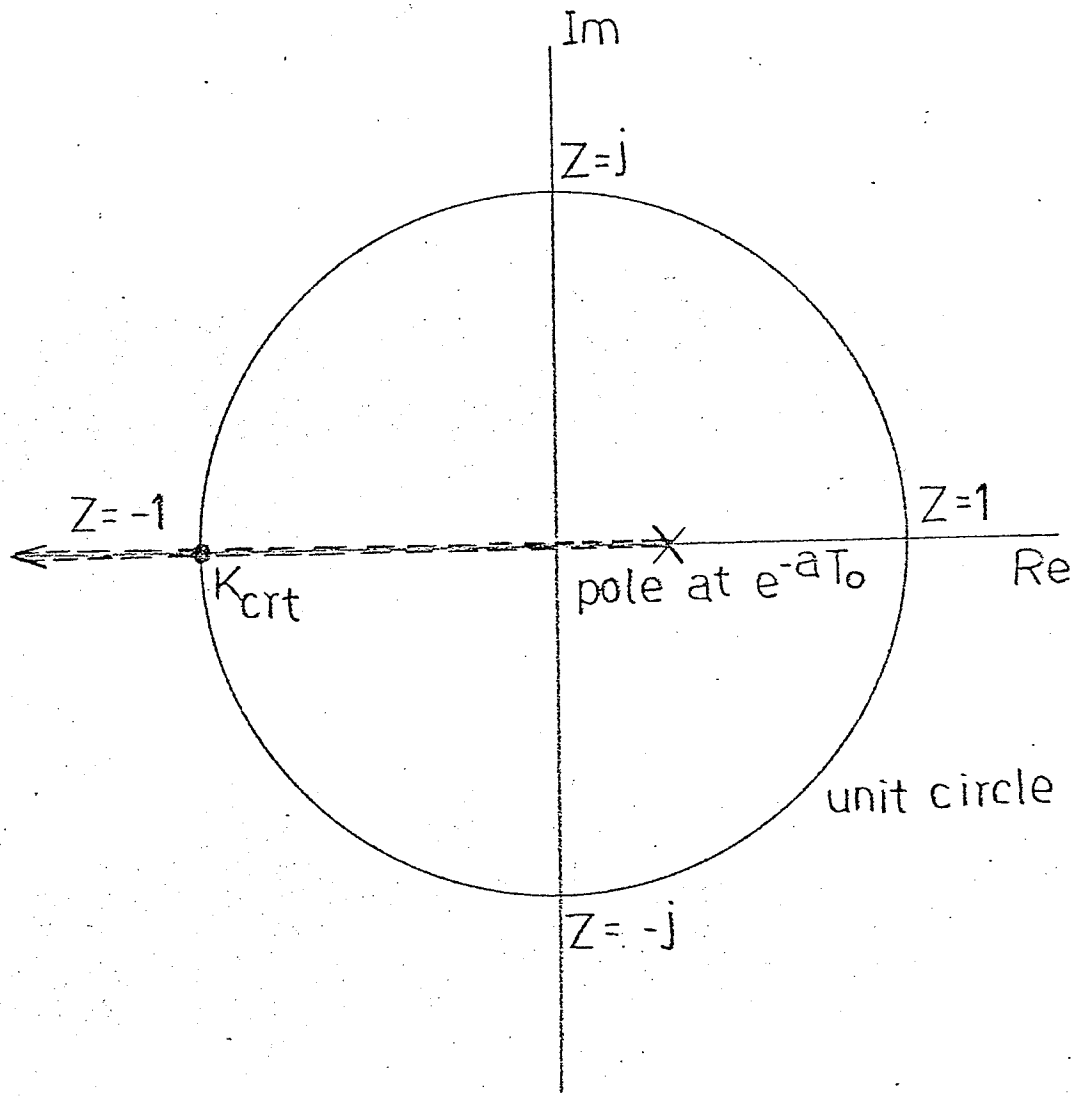


FIGURE 4.2.2 root locus of $G^*(z)$

Eq. (4.6) and (4.9) are two expressions relating the critical gain K_{crit} and the inter-pulse interval T . However, because of their complexity, these expressions cannot be solved analytically to obtain the critical gain K_{crit} and its inter-pulse interval T . They can be obtained by trial and error method, or graphically.

Example I

Consider a first order linear plant which is described by the following differential equation:

$$\dot{y}(t) + 5y(t) = K X(t) \Big|_{t \geq t_K}$$

Assume that $T_0 = 1$, and $E = 1$, it is required to obtain the range of gain, K , for the system so that the system is phase-locked (i.e. $0 < T \leq 1$) and stable.

Solution

The theoretical range of system gain under phase-locked condition is obtained from Eq. (4.6), assuming that the pulse duration Δ equals to zero.

$$K = \frac{5}{T(1-0.5T)}$$

The critical gain for a stable system is obtained from Eq. (4.9)

$$K_c = \frac{735.5 e^{5T}}{(148.41 - e^{5T})}$$

Both results are plotted in Fig. 4.2.3.

From the stability boundary plotted in Fig. 4.2.3 for the case of $a = 5$ and $T_0 = 1$, it is seen that the minimum gain for the system to achieve locking is 10. From Eq. (4.6), the gain K of the system increases

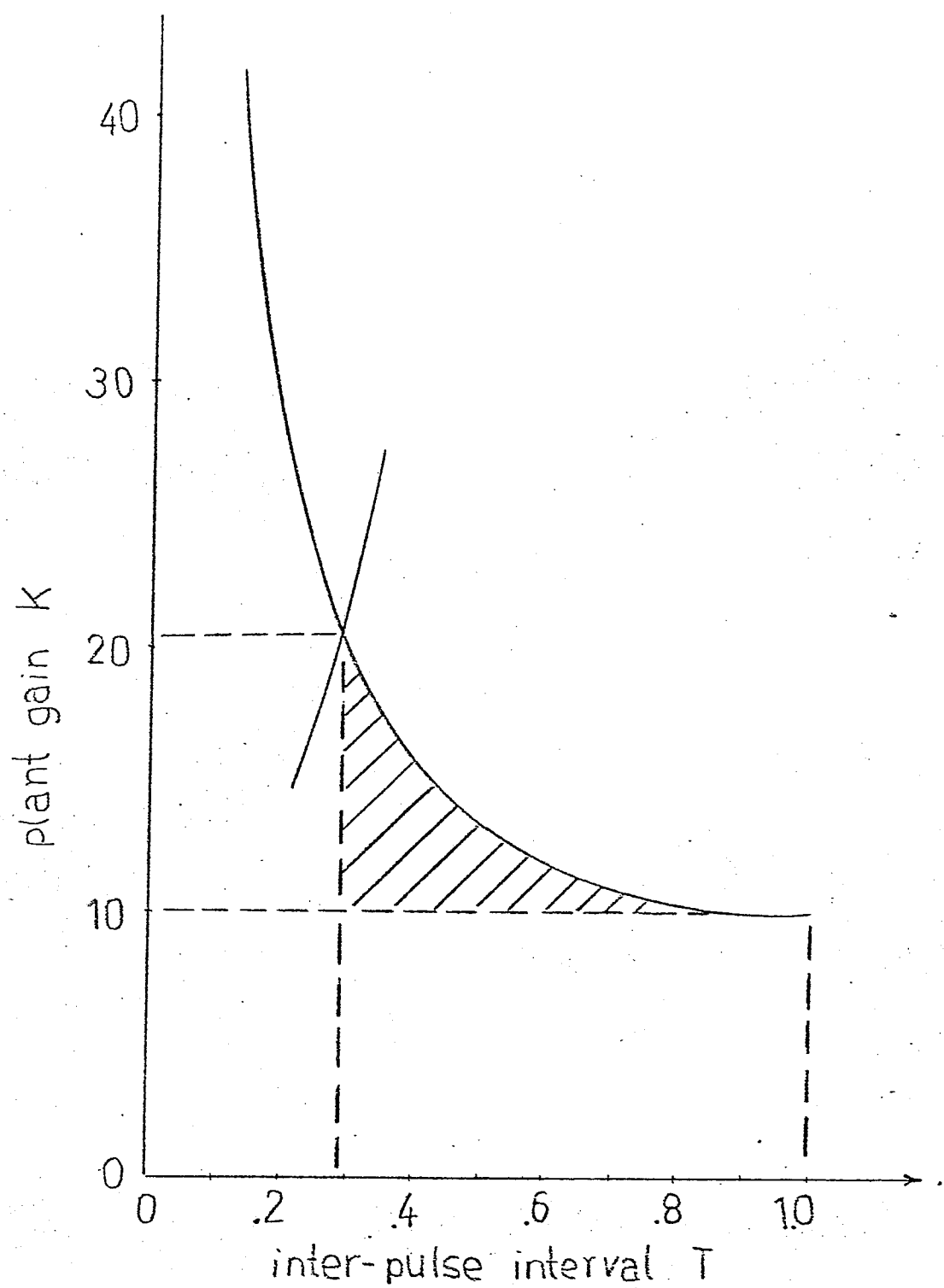
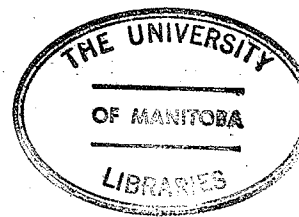


FIGURE 4.2.3 boundary of a stable 1st order system (shaded area)



as the related inter-pulse interval T decreases. The stability limit appears at $T = 0.29$ sec. The maximum allowable gain for this system is 20.4

This system is then simulated on the computer for comparison purposes. The results are shown in the following table.

<u>Gain K</u>	<u>T (Calculated)</u>	<u>T (Simulated)</u>	<u>Phase-Locked</u>
2.50	-	-	No
7.50	-	-	No
10.00	0.900	0.900	Yes
11.00	0.700	0.775	Yes
13.25	0.500	0.525	Yes
20.00	0.300	0.175/0.575	Yes
28.50	0.200	-	No
57.00	0.100	-	No

It is observed that when plant gain is below the minimum value, the system can not be phase-locked. Low plant gain gives low plant output so that the feedback IPFM modulator does not have enough input to initiate pulses at the right time slots. As plant gain increases, the two results are slightly different from each other. The discrepancies are due to the following: in the simulation, pulses with 0.05 second pulse width are used while zero pulse width is assumed in the theoretical analysis. However, when the simulated pulse width is reduced to 0.025 seconds, it is observed that the simulated results are closer to the theoretical values. Finally, when the plant gain increases close to the critical value, the feedback pulses are observed to oscillate around the input pulses. The system loses lock for further increase in gain.

Second Order System(a) Linear plant with two distinct poles

Assume that the linear plant can be described by the following differential equation:

$$\ddot{y}(t) + (a + b)\dot{y}(t) + ab.y(t) = K X(t) \quad |_{t \geq t_K} \quad (4.10)$$

then, the equation can be transformed into two first order differential equations by letting,

$$\begin{aligned} \dot{y}_1(t) + a y_1(t) &= y_2(t) \\ \dot{y}_2(t) + b y_2(t) &= K X(t) \end{aligned} \quad |_{t \geq t_K}$$

Then,

$$\begin{bmatrix} \dot{y}_1 \\ \dot{y}_2 \end{bmatrix} = \begin{bmatrix} -a & 1 \\ 0 & -b \end{bmatrix} \begin{bmatrix} y_1 \\ y_2 \end{bmatrix} + \begin{bmatrix} 0 \\ K \end{bmatrix} X(t)$$

and

$$\underline{A} = \begin{bmatrix} -a & 1 \\ 0 & -b \end{bmatrix}$$

$$\underline{A}^{-1} = \begin{bmatrix} -1/a & -1/ab \\ 0 & -1/b \end{bmatrix}$$

$$\underline{Q} = \begin{bmatrix} 0 \\ K \end{bmatrix}$$

$$\underline{H} = \begin{bmatrix} 1 & 0 \end{bmatrix}$$

The required matrix function $e^{\underline{A}t}$ is evaluated by the Lagrange interpolation formula; i.e.,

$$g(\lambda) = \sum_{j=1}^{n+1} \left(\prod_{\substack{i=1 \\ j \neq i}}^{n+1} \frac{\lambda - \lambda_i}{\lambda_j - \lambda_i} \right) f(\lambda_i)$$

where λ_i 's are the characteristic numbers of the given matrix \underline{A} . and f is a function that depends on the characteristic numbers, and then λ is replaced by the matrix \underline{A} .

$$g(\lambda) = \frac{(\lambda + b) f(-a)}{(b - a)} + \frac{(\lambda + a) f(-b)}{(a - b)}$$

and

$$g(\underline{A}) = \frac{(\underline{A} + b\underline{I}) e^{-at}}{(b - a)} + \frac{(\underline{A} + a\underline{I}) e^{-bt}}{(a - b)}$$

$$\text{Since } g(\underline{A}) = f(\underline{A}) = e^{\underline{A}t}$$

$$e^{\underline{A}t} = \begin{bmatrix} e^{-at} & \frac{e^{-at}}{(b-a)} + \frac{e^{-bt}}{(a-b)} \\ 0 & e^{-bt} \end{bmatrix}$$

and

$$U_{11}(T_o) = e^{-aT_o}$$

Also,

$$\underline{A}^{-2} = \begin{bmatrix} \frac{1}{a^2} & \frac{1}{a^2 b} + \frac{1}{ab^2} \\ 0 & \frac{1}{b^2} \end{bmatrix}$$

From Eq. (3.9)

$$y_{1t_K} = \frac{K(T(\frac{1}{b} - \frac{1}{a}) + \frac{e^{-aT_0}(e^{aT} - 1)}{a^2} - \frac{e^{-bT_0}(e^{bT} - 1)}{b^2})}{a - b - ae^{-bT_0} + be^{-aT_0}} \quad (4.11)$$

From Eq. (3.10), the gain of the system of second order linear plant is:

$$K = \frac{E}{L} \quad (4.12)$$

where

$$L = \frac{y_{1t_K} [\frac{(e^{-aT_0} - 1)b}{a} - \frac{(e^{-bT_0} - 1)a}{b}]}{K(a - b) - \frac{T(a + b - ab(T_0 - \frac{T}{2}))}{a^2 b^2}}$$

$$- \frac{e^{-aT_0}(e^{aT} - 1)}{a^3(a - b)} + \frac{e^{-bT_0}(e^{bT} - 1)}{b^3(a - b)}$$

Hence, Eq. (4.12) gives the theoretical gain of the second order linear plant with two distinct poles for which the system would be phase-locked.

The Schur-Cohn criterion provides a nice analytical method of determining the stability boundary of a phase-locked loop control system. In applying the Schur-Cohn criterion, the characteristic equation in terms of Z for the control system must first be obtained. The stability of a system is dependent upon the location of the roots of the characteristic equation, with all the roots inside the unit circle corresponding to a stable system and with one or more roots outside the unit circle corresponding to an unstable system.

The general Schur-Cohn stability criterion can be simplified in $F(Z)$, the numerator of $1 + K G^*(Z)$, is a quadratic polynomial with real coefficients and the coefficient of Z^2 is unity. In such cases, the necessary

and sufficient conditions for the roots of $F(Z) = 0$ lying inside the unit circle are reduced to⁽¹⁾

$$1. \quad |F(0)| < 1 \quad (4.13a)$$

$$2. \quad F(1) > 0 \quad (4.13b)$$

$$3. \quad F(-1) > 0 \quad (4.13c)$$

The transfer function of the control system is

$$KG(S) = \frac{K(1 - e^{-DS})}{S(S+a)(S+b)} \quad (4.14)$$

The Z transform of Eq. (4.12) is given by

$$\begin{aligned} KG(Z) &= K z \left[\frac{(1 - e^{-DS})}{S(S+a)(S+b)} \right] \\ &= \frac{K(P_1 Z - Q_1)}{ab(a-b)(Z-e^{-aT})(Z-e^{-bT})} \end{aligned} \quad (4.15)$$

where

$$P_1 = ae^{-bT}(e^{bD} - 1) - e^{-aT}(e^{aD} - 1)$$

and

$$Q_1 = e^{-(a+b)T}(a(e^{bD} - 1) - b(e^{aD} - 1))$$

The characteristic equation of this system derived from $1 + KG^*(Z) = 0$ is given by

$$F(Z) = Z^2 - P_2 Z + Q_2 = 0 \quad (4.16)$$

where

$$P_2 = e^{-aT} + e^{-bT} - \frac{K(ae^{-bT}(e^{bD}-1) - be^{-aT}(e^{aD}-1))}{ab(a-b)}$$

⁽¹⁾ See page 241 of 'Digital & Sampled-data control System' by J.T. Tou

and

$$Q_2 = \frac{e^{-(a+b)T_o}(1 + K(b(e^{aD} - 1) - a(e^{bD} - 1))}{ab(a - b)}$$

Applying the stability conditions of Eq. 4.13 leads to the following inequalities:

$$|F(0)| = \frac{e^{-(a+b)T_o}(1 + K(b(e^{aD} - 1) - a(e^{bD} - 1))}{ab(a - b)} < 1 \quad (4.17)$$

$$F(1) = 1 - P_2 + Q_2 > 0 \quad (4.18)$$

$$F(-1) = 1 + P_2 + Q_2 > 0 \quad (4.19)$$

Transposing and simplifying reduces inequality (4.17) to

$$K < \frac{e^{(a+b)T_o}(a - b)}{\frac{a(T_o - T)}{b(e^{-aT_o} - 1) - a(e^{-bT_o} - 1)}} \quad (4.20)$$

In like manner, inequality (4.18) can be reduced to

$$K < \frac{1 - e^{-aT_o} - e^{-bT_o} + e^{-(a+b)T_o}ab(a - b)}{\frac{a(e^{-aT_o} - 1)(e^{-bT_o} - e^{-aT_o}) - b(e^{-bT_o} - 1)(e^{-aT_o} - e^{-aT_o})}{a(e^{-aT_o} + 1)(e^{-bT_o} - e^{-aT_o}) - b(e^{-bT_o} + 1)(e^{-aT_o} - e^{-aT_o})}} \quad (4.21)$$

Also, inequality (4.19) can be simplified to

$$K < \frac{(1 + e^{-aT_o} + e^{-bT_o} + e^{-(a+b)T_o})ab(a - b)}{\frac{-aT_o}{a(e^{-aT_o} + 1)(e^{-bT_o} - e^{-aT_o}) - b(e^{-bT_o} + 1)(e^{-aT_o} - e^{-aT_o})}} \quad (4.22)$$

Hence, the lowest value of inequality (4.20) through (4.22) determines the critical gain K for this stable system.

Example II

Consider a specific second order linear plant which is described by the following differential equation:

$$\ddot{y}(t) + 11 \dot{y}(t) + 30Y(t) = K X(t) \Big|_{t > t_K}$$

Assuming that $T_0 = 1$, and $E = 1$, it is required to obtain the range of gain, K , for the system so that the system is phase-locked (i.e. $0 < T \leq 1$) and stable.

Solution

The theoretical range of system gain under phase-locked condition is obtained from Eq. (4.11) and Eq. (4.12)

$$K = \frac{1}{0.033342T - 0.01665T^2 + 0.000013(e^{6T} - 1) - 0.000046(e^{5T} - 1)} \quad (4.12(a))$$

The three inequalities (4.17) through (4.19) are evaluated by means of digital computer. It is found that inequality (4.18) is always fulfilled provided $0 < T < 1$. Also, the gain obtained from inequality (4.20) is much greater than that obtained from inequality (4.22). Hence inequality (4.22) gives the gain K for this stable system, and

$$K < e^{11T} / (0.198667e^{6T} - 0.16626e^{5T} - 0.000926e^{11T}) \quad (4.22(a))$$

Eq. (4.12(a)) and Eq. (4.22(a)) are both plotted in Fig. 4.2.4.

In Fig. 4.2.4., it is predicted that the system would be stable and phase-locked for the plant gain between 63.775 and 93.50. The maximum allowable gain occurs approximately at $T = 0.405$ seconds. For the gain

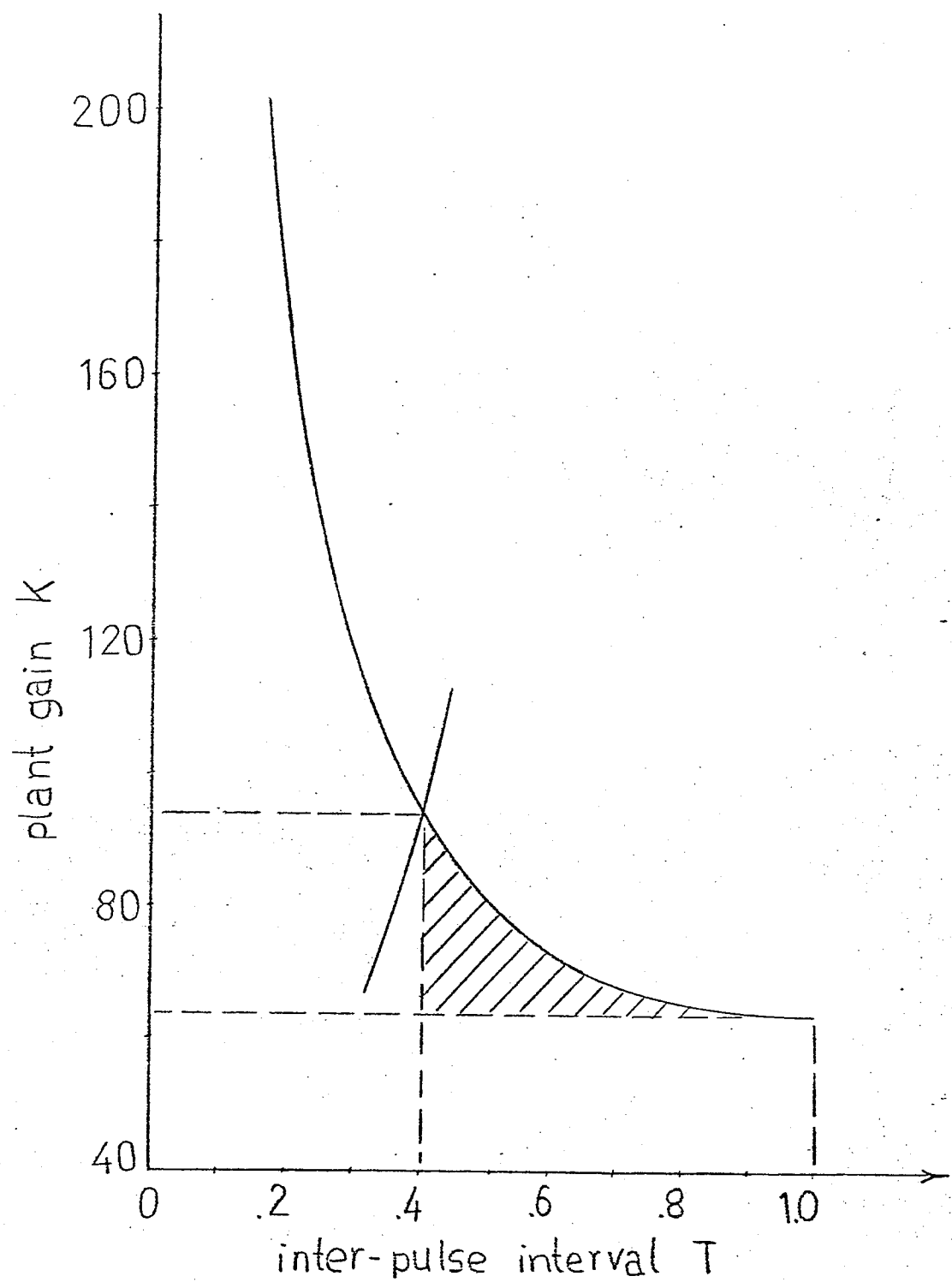


FIGURE 4.2.4 boundary of a stable 2nd order system (shaded area)

above the maximum value, the system would be unstable.

This system is then simulated on computer and the results are compared in the following table.

<u>Gain K</u>	<u>T (Calculated)</u>	<u>T (Simulated)</u>	<u>Phase-Locked</u>
20	--	--	No
40	--	--	No
60	--	--	No
65	0.825	0.775	Yes
76	0.550	0.575	Yes
91	0.420	0.325/0.475	Yes
104	0.350	--	No
166	0.200	--	No
316	0.100	--	No

From the table, the results are satisfactory at low plant gain and the system is not phase-locked when the plant gain is below the minimum value. However, there are discrepancies between the two results when the system is phase-locked. These are mainly because the pulse width of 0.05 seconds is used in the simulation. Improvements in the results can be seen if smaller pulse width is simulated. Also, the feedback pulses oscillate at above the critical gain and the system loses lock for gain beyond the critical values.

(b) Linear plant with a multiple pole of order two

The linear plant is described by the following differential equation:

$$\ddot{y}(t) + 2a\dot{y}(t) + a^2y(t) = K X(t) \Big|_{t \geq t_K} \quad (4.23)$$

Transforming into two first order differential equation yields

$$\begin{array}{l} \dot{y}_1(t) + a y_1(t) = y_2(t) \\ \dot{y}_2(t) + a y_2(t) = K X(t) \end{array} \quad \left|_{t > t_K} \right.$$

or,

$$\begin{bmatrix} \dot{y}_1 \\ \dot{y}_2 \end{bmatrix} = \begin{bmatrix} -a & 1 \\ 0 & -a \end{bmatrix} \begin{bmatrix} y_1 \\ y_2 \end{bmatrix} + \begin{bmatrix} 0 \\ K \end{bmatrix} X(t) \quad \left|_{t \geq t_K} \right.$$

Then,

$$\underline{A} = \begin{bmatrix} -a & 1 \\ 0 & -a \end{bmatrix}$$

$$\underline{A}^{-1} = \begin{bmatrix} -\frac{1}{a} & \frac{1}{a^2} \\ 0 & -\frac{1}{a} \end{bmatrix}$$

$$\underline{A}^{-2} = \begin{bmatrix} \frac{1}{a^2} & \frac{2}{a^3} \\ 0 & \frac{1}{a^2} \end{bmatrix}$$

$$\underline{Q} = \begin{bmatrix} 0 \\ K \end{bmatrix}$$

$$\underline{H} = [1 \quad 0]$$

To construct the Lagrange interpolation $h(\lambda)$, consider the partial fraction expansion of rational function

$$\frac{h(\lambda)}{m(\lambda)} = \frac{h(-a)}{(\lambda+a)^2} + \frac{h'(-a)}{(\lambda+a)}$$

where

$$h(-a) = \left. \frac{h(\lambda)(\lambda+a)^2}{m(\lambda)} \right|_{\lambda = -a}$$

$$h'(-a) = \left. \frac{d}{d\lambda} \frac{h(\lambda)(\lambda+a)^2}{m(\lambda)} \right|_{\lambda = -a}$$

On the spectrum of A,

$$h(-a) = f(-a) = e^{-at}$$

$$h'(-a) = t e^{-at}$$

$$h(\lambda) = e^{-at} + (\lambda + a)t e^{-at}$$

Replacing λ by A gives $e^{\underline{A}t}$

$$g(\underline{A}) = e^{\underline{A}t} = h(\underline{A}) = \underline{I} e^{-at} + (\underline{A} + a \underline{I}) e^{-at}$$

$$e^{\underline{A}t} = \begin{bmatrix} e^{-at} & t e^{-at} \\ 0 & e^{-at} \end{bmatrix}$$

$$U_{11}(T_0) = e^{-aT_0}$$

From Eq. (3.9),

$$y_1 t_K = \frac{K[aT_0 + (2 + aT_0)e^{-aT_0} - (2 + aT_0 - aT)e^{-a(T_0 - T)}]}{a^3 [1 - (1 + aT_0)e^{-aT_0}]}$$

(4.24)

From Eq. (3.10), the gain of the system of second order linear plant with a multiple pole is

$$K = \frac{E}{L}$$

where $L = \frac{-y_1 e^{-aT_o} (2 + aT_o)}{a K} + \frac{a^2 T_o (T_o - \frac{T}{2}) - e^{-aT_o} (aT_o + 3) - 2aT_o + e^{-a(T_o - T)} (aT_o - aT_o + 3)}{a^4}$

(4.25)

Hence, Eq. (4.25) gives the theoretical gain of the second order linear plant with a multiple pole of order two so that the system would be phase-locked.

In order to obtain the stability boundary of the controlled system, it is necessary to obtain the transfer function of the sampled-data system.

$$K G(S) = \frac{K(1 - e^{-DS})}{S(S + a)^2} \quad (4.26)$$

The Z transform of Eq. (4.12) is given by

$$K G(Z) = \frac{K e^{-aT_o} (P_3 Z + Q_3)}{(Z - e^{-aT_o})^2 a^2}$$

where

$$P_3 = e^{-a(T_o - T)} (1 + aT) - aT_o - 1$$

$$Q_3 = e^{-aT_o} + e^{-aT} (aT_o - 1 - aT)$$

The characteristic equation of this system derived from $1 + K G^*(Z)$ is given by

$$F(Z) = Z^2 + P_4 Z + Q_4 = 0 \quad (4.27)$$

where

$$P_4 = (K P_3 a^{-2} - 2) e^{-aT_o}$$

$$Q_4 = e^{-2aT_o} + K e^{-aT_o} Q_3 a^{-2}$$

Since the characteristic equation of the controlled system is a quadratic polynomial, Eq. (4.13) is applicable. Then,

$$|F(0)| = e^{-2aT_o} (1 + K(1 + e^{-aT_o} (aT_o - 1 - aT))) < 1 \quad (4.28)$$

$$F(1) = 1 + P_4 + Q_4 > 0 \quad (4.29)$$

$$F(-1) = 1 - P_4 + Q_4 > 0 \quad (4.30)$$

Transposing and simplifying reduces inequality (4.28) to

$$K < \frac{a^2 (e^{-aT_o} - 1)}{1 + e^{-aT_o} (aT_o - 1 - aT)} \quad (4.31)$$

In like manner, inequality (4.29) can be reduced to

$$K < \frac{a^2 (e^{-aT_o} - 2 + e^{-aT_o})}{(1 - e^{-aT_o}) + a(1 - e^{-aT_o}) - e^{-aT_o} (1 + aT_o) (e^{-aT_o} - 1)} \quad (4.32)$$

Also, inequality (4.30) becomes

$$K < \frac{a^2 (e^{-aT_o} + 2 + e^{-aT_o})}{-(1 + e^{-aT_o}) - a(1 + e^{-aT_o}) + e^{-aT_o} (1 + aT_o) (e^{-aT_o} + 1)} \quad (4.33)$$

Hence, the lowest value of inequality (4.31) through (4.33) determines the critical gain for this stable system.

Example III

Consider a second order linear plant which is described by the following differential equation:

$$\ddot{y}(t) + 10\dot{y}(t) + 25y(t) = K X(t) \Big|_{t > t_K}$$

Assuming that $T_0 = 1$, and $E = 1$, it is required to obtain the range of gain, K , for the system so that the system is phase-locked (i.e. $0 < T \leq 1$) and stable.

Solution

The theoretical range of gain under phase-locked conditions is obtained from Eq. (4.24) and Eq. (4.25)

$$K = (-0.000089 + 0.0236T - 0.02T^2 + 0.000089 e^{5T} - 0.000055Te^{5T})^{-1} \quad (4.25(a))$$

The three inequalities (4.28) through (4.30) are evaluated by means of a digital computer. It is founded that inequality (4.29) is always fulfilled. The gain evaluated from inequality (4.31) is greater than that obtained from inequality (4.33). Hence, inequality (4.33) provides the critical gain for a stable system; i.e.

$$K < e^{5T} / (0.0384 + 0.1986T - 0.001597 e^{5T}) \quad (4.33(a))$$

Eq. (4.25(a)) and Eq. (4.33(a)) are both plotted in Fig. 4.2.5. It is predicted that the system would be phase-locked and stable at a gain between 118 and 129. These results are compared with that simulated on digital computer in the following table:

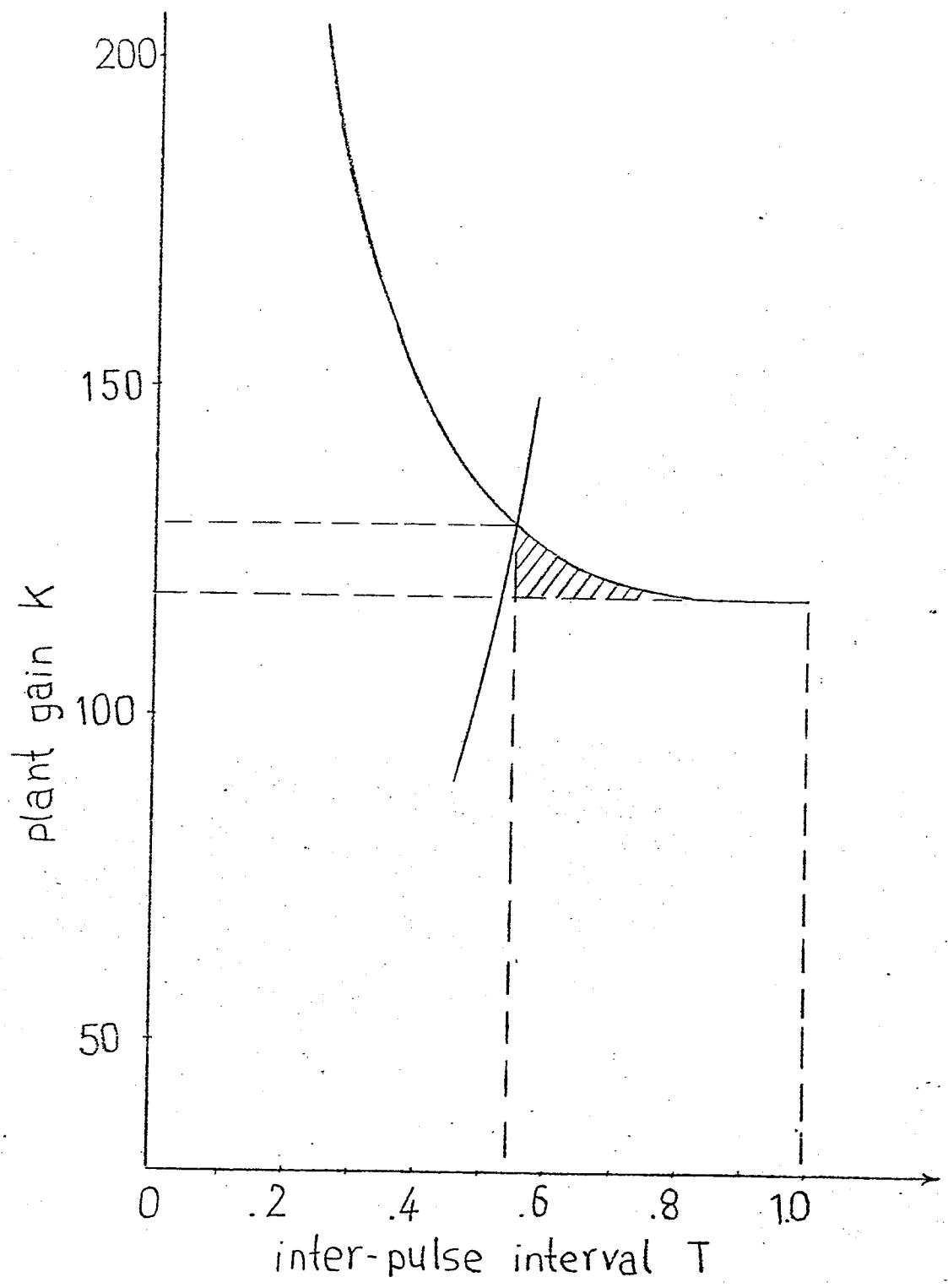


FIGURE 4.2.5 boundary of a stable 2nd order system (shaded area)

<u>System Gain</u>	<u>Predict T(sec)</u>	<u>Simulated T(sec)</u>	<u>Phase-Locked</u>
20	---	---	No
50	---	---	No
100	---	---	No
120	0.73	0.525	Yes
128	0.55	0.425	Yes
150	0.4	---	No
200	0.26	---	No

The discrepancies between the T's are similar to those cited earlier. However, the comparison shows that the predicted results agree with those from simulations.

CHAPTER 5

SUMMARY AND CONCLUSION

In this thesis, the locking conditions for steady state operation of a phase-locked loop control system are analyzed in the time domain using the state variable approach. This analysis is done by assuming that the system is locked and in steady state operation. In other words, the feedback pulses are initiated at the predetermined inter-pulse interval T when the required plant gain is applied, and the system response is periodic with period T_0 . This is then used to establish the locking conditions for the system.

These locking conditions show that the system does not lock for very low gains, and locks for higher gains. At very high gain, however, simulations show instability of the system, and the feedback pulses are observed to oscillate about their calculated positions. This leads to the stability investigations.

It is observed that, for small oscillation of the feedback pulses around their predicted positions, the stability of the system is equivalent to the stability of a sampled-data system with a special hold device. The concept of using equivalent systems simplifies the investigation of stability. The sampled-data system with a special hold device is analyzed by using Z transform techniques. Two methods of determining the stability of the sampled-data system are discussed. The root locus method provides a graphical means of determining the stability and the simplified Schur-Cohn criterion provides an analytical tool for testing the stability of second order systems.

The simulations confirm the theoretical results. The theory shows

that, for any phase-locked loop control system, there is a range of plant gain for the system to be in phase-locked state. From the simulations of first and second order systems, it is shown that when the gain is too low, the system cannot be phase-locked because the feedback modulator does not have enough time to initiate pulses. On the other hand, when the gain is too high, the steady state solution becomes unstable because more than one pulse is generated in one time slot. In conclusion, the proposed phase-locked loop control system can adequately be described by the methods outlined in this thesis.

BIBLIOGRAPHY

- C1. Clark, J.P.C., "An analysis of pulse frequency modulated control systems", Ph.D. Dissertation, University of Washington, Seattle, April, 1965.
- F1. Farrenkopf, R.L., Sabroff, A.E. and Wheeler, P.C., "Integral pulse frequency on-off control", AIAA Reprint 63-328; August, 1963.
- G1. Gantmacher, "Matrix theory", Vol. 1, pp. 116-124. Chelsea publishing Co., New York, 1959.
- G2. Gille, Pelegrin, Decaulne, "Feedback control systems", McGraw-Hill, New York, 1959.
- L1. Li, C.C., "Integral pulse frequency modulated control systems", Ph.D. Dissertation, Northwestern University; August, 1961.
- M1. Moore, A.W., "Phase-locked loops for motor-speed control", IEEE Spectrum, Vol. 10, pp. 61-67, April 1973.
- M2. Meyer, A.U., "Pulse frequency modulation and its effects in feedback control systems", Ph.D. Dissertation, Northern University, August, 1961.
- M3. Murphy, W.L. and West, K.L., "The use of pulse frequency modulation for adaptive control", Proc. of the N.E.C., Chicago, Illinois, Vol. 18, pp. 271-277; October 8, 1962.
- T1. Tou, J.T., "Digital and sampled-data control systems", McGraw-Hill, New York, 1959.